

Global spatial risk assessment of sharks under the footprint of fisheries

A list of authors and their affiliations appears in the online version of the paper.

Effective ocean management and the conservation of highly migratory species depend on resolving the overlap between animal movements and distributions, and fishing effort. However, this information is lacking at a global scale. Here we show, using a big-data approach that combines satellite-tracked movements of pelagic sharks and global fishing fleets, that 24% of the mean monthly space used by sharks falls under the footprint of pelagic longline fisheries. Space-use hotspots of commercially valuable sharks and of internationally protected species had the highest overlap with longlines (up to 76% and 64%, respectively), and were also associated with significant increases in fishing effort. We conclude that pelagic sharks have limited spatial refuge from current levels of fishing effort in marine areas beyond national jurisdictions (the high seas). Our results demonstrate an urgent need for conservation and management measures at high-seas hotspots of shark space use, and highlight the potential of simultaneous satellite surveillance of megafauna and fishers as a tool for near-real-time, dynamic management.

Industrialized fishing is a major source of mortality for large marine animals (marine megafauna)^{1–6}. Humans have hunted megafauna in the open ocean for at least 42,000 years⁷, but international fishing fleets that target large, epipelagic fishes did not spread into the high seas until the 1950s⁸. Prior to this, the high seas constituted a spatial refuge that was largely free from exploitation, as fishing pressure was concentrated on continental shelves^{3,8}. Pelagic sharks are among the widest-ranging vertebrates, with some species exhibiting annual migrations on the ocean-basin scale⁹, long term trans-ocean movements¹⁰ and/or fine-scale site fidelity to preferred shelf and open ocean areas^{5,9,11}. These behaviours could cause extensive spatial overlap with different fisheries that exploit regions ranging from coastal areas to the deep ocean. On average, large pelagic sharks account for 52% of all of the identified shark catch worldwide, from both shark-targeting fisheries and as bycatch¹². Regional declines in abundance of pelagic sharks have previously been reported^{13,14}, but it is unclear whether exposure to high levels of fishing effort extends across ocean-wide population ranges and overlaps areas of the high seas in which sharks are most abundant^{5,13}. The conservation of pelagic sharks—the management of which on the high seas is currently limited^{12,15,16}—would benefit greatly from a clearer understanding of the spatial relationships between the habitats of sharks and active fishing zones. However, obtaining unbiased estimates of the distributions of sharks and fishing effort is complicated by the fact that most data on pelagic sharks come from catch records and other fishery-dependent sources^{4,15,16}.

Here we provide a global estimate of the extent of overlap in the use of space between sharks and industrial fisheries. This estimate is based on analysis of the movements of pelagic sharks tagged with satellite transmitters in the Atlantic, Indian and Pacific Oceans, together with the movements of fishing vessels that are monitored globally by the automatic identification system (AIS), which was developed as a vessel safety and anti-collision system (Methods). Our study focuses on 23 species of large pelagic sharks that occupy oceanic and/or neritic habitats, which span a broad distribution from cold-temperate to tropical waters (Supplementary Table 1). All of these species face some level of fishing pressure from coastal, shelf and/or high-seas fisheries: the International Union for the Conservation of Nature (IUCN) Red List assesses almost two-thirds of these species as being endangered (26%) or vulnerable (39%), and a further quarter as near-threatened (26%) (Supplementary Table 2). Although regional-fisheries management

organizations are tasked with the management of sharks in the high seas, little or no management is in place for most species^{3,5,12–18}.

Movement patterns of sharks and fishing vessels

The 11 shark species (or taxa groups) that accounted for 96% of the 1,804 satellite tags that were deployed are among the largest of shark species: blue sharks (*Prionace glauca*); shortfin mako sharks (*Isurus oxyrinchus*); tiger sharks (*Galeocerdo cuvier*); salmon sharks (*Lamna ditropis*); whale sharks (*Rhincodon typus*); white sharks (*Carcharodon carcharias*); oceanic whitetip sharks (*Carcharhinus longimanus*); porbeagle sharks (*Lamna nasus*); silky sharks (*Carcharhinus falciformis*); bull sharks (*Carcharhinus leucas*); and hammerhead sharks (*Sphyrna* spp.) (Supplementary Tables 3–5). Movement patterns indicated that multiple species aggregated within the same major oceanographic features (Fig. 1), such as the Gulf Stream (blue sharks, shortfin mako sharks, tiger sharks, white sharks and porbeagle sharks), the California Current (blue sharks, shortfin mako sharks, white sharks and salmon sharks) and the East Australian Current (blue sharks, shortfin mako sharks, tiger sharks, white sharks and porbeagle sharks), (Extended Data Fig. 1; see ‘Supplementary results and discussion, section 2.1’ in the Supplementary Information). The global relative density map (Fig. 2a) reveals distribution patterns of pelagic sharks and the locations of space-use hotspots (defined here as areas with ≥ 75 th percentile of weighted daily location density) (Methods). Major space-use hotspots of tracked pelagic sharks in the Atlantic Ocean were in the Gulf Stream and its western approaches, the Caribbean Sea, the Gulf of Mexico and around oceanic islands such as the Azores (Fig. 2a, Supplementary Table 6). In the Indian Ocean, space-use hotspots were evident in the Agulhas Current, Mozambique Channel, the South Australian Basin and northwest Australia, and in the Pacific Ocean, space-use hotspots were in the California Current, Galapagos Islands and around New Zealand. Although, as expected, tagging sites occurred in some space-use hotspots (as tagging rates are inherently higher in hotspots), we also identified space-use hotspots in which no tagging sites occurred in the North Atlantic Ocean (outer Gulf Stream, Charlie Gibbs Fracture Zone, western European shelf edge and the Bay of Biscay), the Indian Ocean (southern Madagascar, the Crozet and Amsterdam Islands, and the South Australian Basin) and the Pacific Ocean (Alaska Current, outer California Current, the white shark ‘café’ area, halfway between Baja California and Hawaii¹¹, North Equatorial Current, Clipperton Island

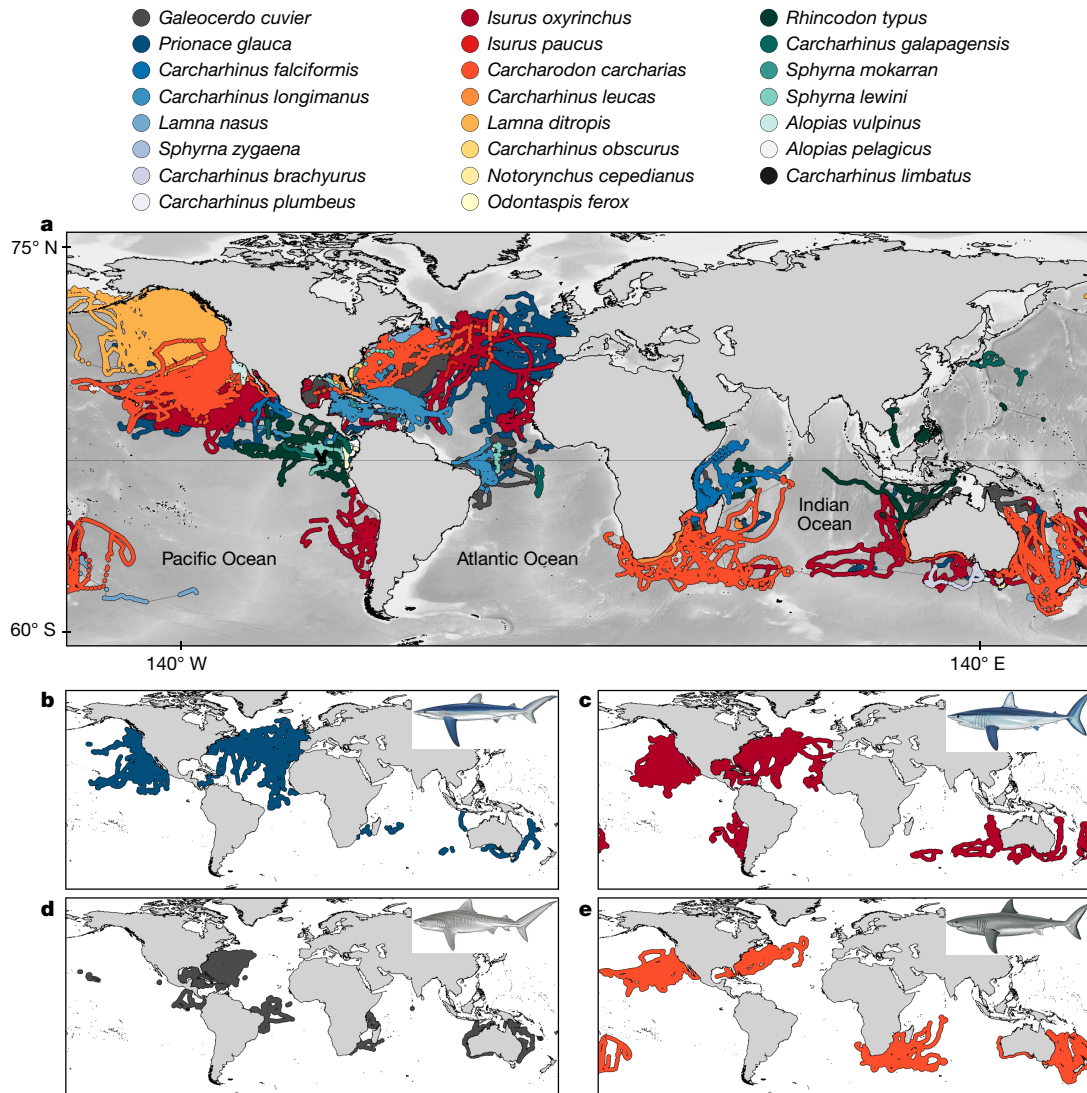


Fig. 1 | Movements of oceanic and neritic pelagic sharks. a, Daily state-space model locations, estimated from locations obtained via satellite transmitters deployed on 1,681 sharks from 23 species between 2002 and 2017. **b–e**, Extent of the space use areas of individual shark species are

illustrated for the species with the greatest numbers of tags deployed across multiple ocean regions: blue shark (**b**), shortfin mako shark (**c**), tiger shark (**d**) and white shark (**e**). Shark images created by M. Dando.

and Kermadec Islands) (Extended Data Fig. 1). There was consistency between our fine-scale identification of hotspots of space use by sharks, and the coarse-scale species richness hotspots of oceanic predators estimated from fishery-dependent catch data⁴ (see ‘Supplementary results and discussion, section 2.1’ in the Supplementary Information).

To determine the extent to which hotspots of space use by sharks fall under the footprint of global industrialized fisheries, we mapped the movements of fishing vessels that carry AIS transmitters (estimated to be fitted on 50–75% of active vessels that are over 24 m in length)^{19–23}. First, we mapped the mean annual and mean monthly fishing effort (in days) of AIS-equipped fishing vessels that use various types of fishing gear^{19,20} for the period 2012–2016 (Extended Data Fig. 2, Methods), and then mapped the estimated global fishing effort of drifting pelagic longline and purse seine vessels separately (as these two types of gear catch the majority of pelagic sharks^{12,15}) (Fig. 2b, Extended Data Fig. 2). The global distribution map of longline fishing effort identifies several large-scale areas that are used heavily, such as the North Atlantic Ocean, southwest Indian Ocean, and the central equatorial and northwest regions of the Pacific Ocean (Fig. 2b, Extended Data Figs. 1, 2). There were also areas in which industrial longline activity appeared sparse; for example, the central and southwest North Atlantic Ocean, northeast Pacific Ocean and northern Indian Ocean. We focused our

detailed analysis of shark overlap with that of longline fishing effort, as it is this gear that catches most pelagic sharks globally¹⁵ and because most of the other types of gear used by the AIS-equipped fishing vessels represented in the dataset do not target or generate abundant bycatch of pelagic sharks^{19,20} (see ‘Supplementary results and discussion, section 2.2’ in the Supplementary Information). The number of longline-fishing-effort days estimated for the Atlantic Ocean using AIS data was positively correlated with the number of observed baited longline hooks (observed hooks) that were deployed in the Atlantic Ocean (Spearman’s $r = 0.182$, $P = 0.008$; $n = 241$) (Methods), which confirms that longline-fishing-effort days based on AIS data are indicative of actual fishing effort^{19,20}.

Spatial overlap of sharks and fishing effort

To explore the spatial heterogeneities of sharks and vessels, we used generalized additive models to determine how the relative density of location estimates for sharks and the distribution of longline-fishing effort were affected by environmental covariates (Methods, Supplementary Table 7). Distributions of the density of pelagic sharks and of the fishing effort of pelagic longline vessels were best explained by the same drivers: both demonstrated strong relationships with habitat types that are characterized by surface and subsurface temperature

gradients (fronts²⁴ and thermoclines) and/or high primary productivity (Extended Data Fig. 3, Supplementary Table 8, see ‘Supplementary results and discussion, section 2.3’ in the Supplementary Information). The similar environmental drivers that we identified between shark density and fishing effort predict a high spatial overlap between sharks and fishers: sharks are known to aggregate in biologically productive features (such as fronts) to enhance their foraging opportunities^{5,6,24}, a behaviour that fishers exploit to increase their chances of making higher catches of commercially valuable epipelagic fishes (including sharks)^{5,6}.

We calculated the spatial overlap of tracked sharks with longline-fishing effort for a mean month within the datasets (Methods). Overlap was defined as the spatial co-occurrence of sharks and fishing effort within a $1^\circ \times 1^\circ$ grid cell in an average month (Methods) (for grid-cell size analysis, see Extended Data Fig. 4, Supplementary Table 9, ‘Supplementary results and discussion, section 2.4’ in the Supplementary Information). The overlap between the space use of tracked sharks and fishing effort was dominated by pelagic longline gear (Fig. 2; compare the longline distribution in Fig. 2b with the distribution of fishing effort of all AIS-equipped fishing vessels in Extended Data Fig. 2a). Globally, the distribution of longline-fishing activity in the dataset overlapped 24% of the mean monthly space use of tracked sharks at the $1^\circ \times 1^\circ$ scale (mean \pm s.d. monthly overlap, $23.7\% \pm 32.7$; median, 4.5%; $n = 1,681$ tracks). This estimate is unlikely to be biased by the fact that a majority of our tags were deployed in the northwest Atlantic Ocean or northeast Pacific Ocean, because there was relatively low AIS-monitored longline-fishing effort in both regions (Figs. 1a, 2a–c). Across the four regions in which the majority of sharks were tracked, mean monthly spatial overlap of the 11 most-frequently tracked species or taxa groups with longline-fishing effort was 8% (eastern Pacific Ocean), 24% (Oceania), 37% (North Atlantic Ocean) and 38% (southwest Indian Ocean) (Supplementary Table 10). Differences in the overlap patterns between space use and fishing effort between ocean regions—and for species within regions—were not driven by the numbers of tags that we deployed (see ‘Supplementary results and discussion, section 2.1’ in the Supplementary Information). Overlap varied across species and oceans, which reflects the heterogeneous distributions of both space use by sharks and longline fishing activity (Extended Data Figs. 6, 7). For example, monthly spatial overlap with fishing effort averaged across all oceans ranged from 49% for the blue shark to 1.3% for the salmon shark. Between oceans, the overlap of space use by blue sharks (the pelagic shark that is most-commonly caught by open-ocean longline fleets¹⁷) with fishing effort was 76% in the North Atlantic Ocean, which decreased to 14% in the eastern Pacific Ocean (median overlap values are given in Supplementary Tables 10, 11).

To estimate the potential exposure of sharks in different regions of the oceans to longline-fishing effort, we calculated the mean monthly fishing effort to which individual sharks were exposed in each grid cell that the shark occupied during a corresponding month, standardized to account for variations in the durations of individual tracks; this is hereafter referred to as the fishing exposure index (FEI) (Methods). As expected, across all oceans and species sharks were exposed to highly variable longline-fishing effort (Supplementary Table 10). Given this, we tested whether the FEI was indicative of actual sharks captured and landed by fisheries. We compared the median monthly individual-species FEI for shark species in the North Atlantic Ocean (the ocean for which we had the most species and tracks) with official records from the Food and Agriculture Organization of the United Nations (FAO) regarding the mean annual landings of these species in the North Atlantic Ocean (Methods). We found a significant positive relationship between these FAO landings data and the individual-species mean FEI (linear regression, $r^2 = 0.45$, $n = 8$ species (or taxa group), $F = 6.72$, $F_{0.05(1),1.7} = 5.59$, $P < 0.05$) (Extended Data Fig. 5), which implies that the index reflects fishing-induced shark mortality.

Hotspots of spatial overlap of the relative density of sharks with longline-fishing effort were evident, for example, in the Gulf Stream and stretching eastward to the Azores, on the western European shelf

edge, in the west African upwelling, in the California Current (and white shark café¹¹), in the Agulhas Current, on the southern Great Barrier Reef, and in New Zealand shelf waters (Fig. 2c). This demonstrates that, globally, high levels of fishing effort are focused on extensive hotspots of space use by sharks (Supplementary Tables 6, 12). Nonetheless, substantial areas of the high seas that are used by pelagic sharks may exist that are largely free from the AIS-monitored fishing activity of longline and purse seine vessels, which could be targeted for shark conservation measures (see ‘Supplementary results and discussion, section 2.7’ in the Supplementary Information). Identifying such areas can only be addressed using fishery-independent distributions (as are presented here). However, a general characteristic of large areas with low levels of longline-fishing activity was lower densities of sharks (<75th percentile of relative density) (Fig. 2a), which indicates that sharks were not remaining in these areas but were rather moving through them—potentially as part of foraging excursions or migrations for reproduction^{9,11}. The lower relative density of sharks in these areas suggests lower productivity—which is supported by our modelling results (model 1) (Extended Data Fig. 3)—and, consequently, poorer fishing opportunities (which may explain the apparent low levels of fishing effort in these areas). The results also show that very few large hotspots of space use by pelagic sharks occurred in areas that are free of AIS-equipped fishing vessels, particularly those with longline and purse seine gear (Fig. 2c, Extended Data Fig. 2c, d).

Determining the spatial risk to sharks from fishing

The extent of spatial overlap between the relative density distribution of sharks and longline-fishing effort indicates which species are more at risk from fishing, and how this risk is distributed (Fig. 3). Because we demonstrate that a large proportion of shark mortality related to fishing (as represented by landings) is related to longline-fishing effort in areas of shark space use, it follows that sharks that have both a high overlap with fishing effort and a high FEI (greater susceptibility) will be at a greater risk of capture than those with low overlap and low FEI (Fig. 3). We found the main commercially valuable pelagic sharks were grouped within the highest potential risk zone in the North Atlantic Ocean and eastern Pacific Ocean (blue sharks and shortfin mako sharks) (Fig. 3a, b; see ‘Supplementary results and discussion, section 2.5’ in the Supplementary Information for significance tests, and for results for the other species). In the North Atlantic Ocean, shortfin mako sharks and blue sharks were at a significantly greater risk compared to other tracked sharks, because their mean monthly space use overlap (62% (median, 71%) and 76% (median, 81%), respectively) co-occurred with a high mean FEI (Fig. 3a, Extended Data Figs. 6, 7, Supplementary Table 10). However, exposure risk varied between oceans because, although the spatial overlap with fishing effort of blue sharks remained relatively high in the southwest Indian Ocean, and for blue sharks and shortfin mako sharks in Oceania (mean, 18–47%; median, 11–33%; Supplementary Table 10), individual-species FEI means were lower in areas of overlap in these regions (Fig. 3a, c, d).

Among sharks that are generally considered to be of less commercial value (including tiger sharks and bull sharks), we found that risk from longlines was high in some—but not all—regions. Bull sharks used spatially limited near-shore habitats in tropical regions within the southwest Indian Ocean: in these areas, they were at increased risk owing to high mean overlap with fishing effort (94%) and high mean FEI (Fig. 3c, Supplementary Table 10). This greater susceptibility could lead to high localized catches, which (if replicated elsewhere) could explain why bull sharks are one of the ten most-commonly traded species in the Hong Kong fin market²⁵. By contrast, tiger sharks were exposed to lower overlap and lower mean FEI in all ocean areas except for Oceania, where they were within the highest potential-risk zone (Fig. 3a–d, see ‘Supplementary results and discussion, sections 2.5, 2.6’ in the Supplementary Information).

High risk was evident for internationally protected sharks under the Convention on International Trade in Endangered Species (CITES) Appendix II and regional-fisheries management organization

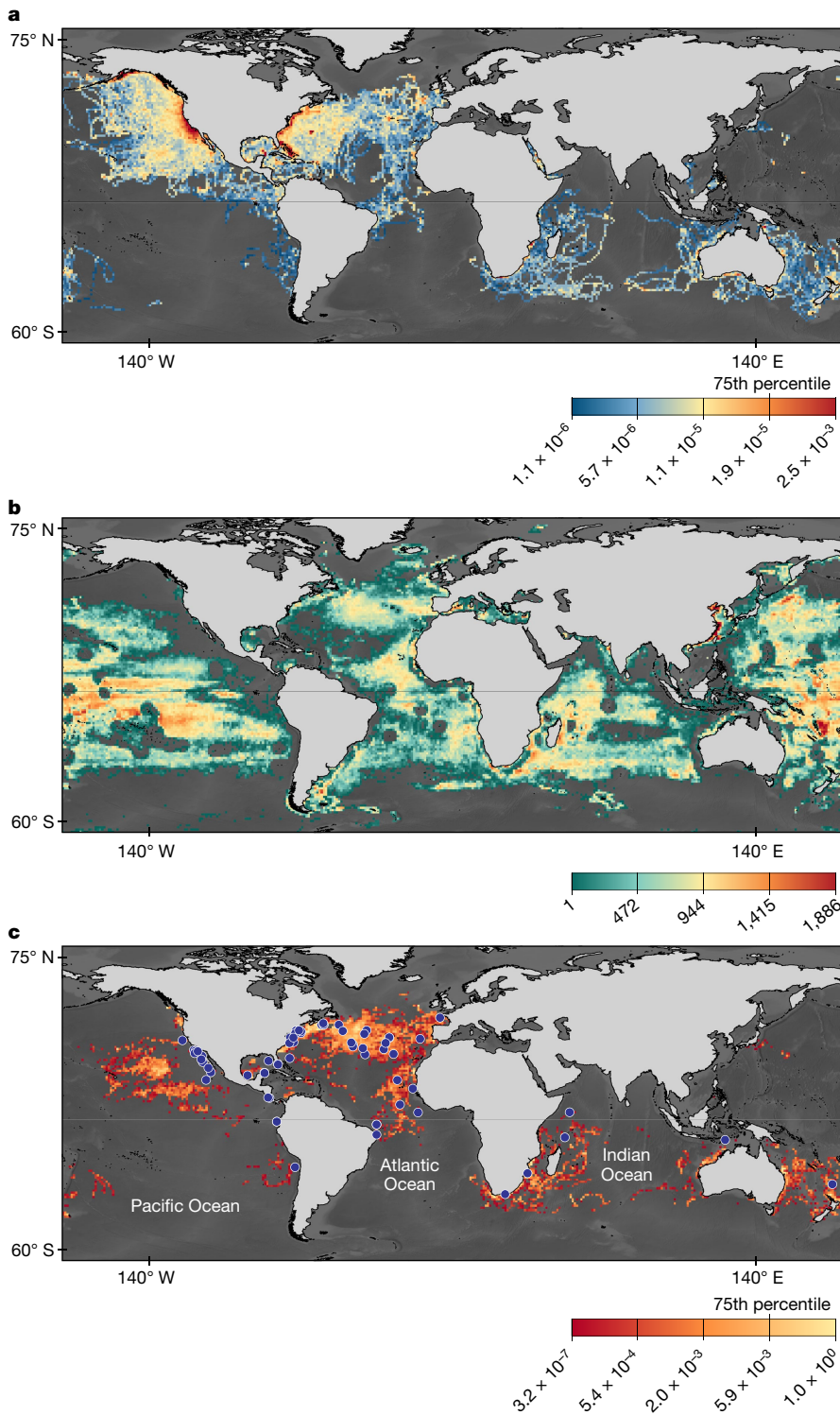


Fig. 2 | Spatial distributions and overlap of sharks and longline fishing vessels. **a**, Relative density of sharks. Distribution of the mean monthly weighted, normalized location density of tracked sharks in $1^\circ \times 1^\circ$ grid cells (shark hotspots were defined by cells with ≥ 75 th percentile of relative density). **b**, Number of days fishing. Mean annual distribution of fishing effort (mean days per grid cell) of AIS-tracked longline fishing vessels in 2012–2016 (see Methods). **c**, FEI. Distribution of the mean monthly overlap and level of fishing effort (in days) that sharks were exposed to in overlapping areas for all species within $1^\circ \times 1^\circ$ grid cells (see Methods). Hotspots of spatial overlap of shark density and fishing effort were defined as cells with ≥ 75 th percentile of mean FEI. Blue circles denote locations at which tagged sharks were caught by commercial fishers, mainly using pelagic longlines and coastal nets.

regulations. The porbeagle shark (global status of endangered on the IUCN Red List) and white shark (global status of vulnerable on the IUCN Red List) have low population sizes compared to historic levels (Supplementary Table 2). In the North Atlantic Ocean and Oceania, we found that the porbeagle shark occurred in the highest-risk zone (Fig. 3a, d), which indicates a high potential for mortality as a result of incidental bycatch. White sharks were in the highest-risk zone in all oceans in which they were tracked, with a mean spatial overlap with fishing effort that ranged from 15% (median 13%) in the east Pacific Ocean to 64% (median 65%) in the southwest Indian Ocean—except for the North Atlantic Ocean, in which their mean FEI was just below the average FEI for all species (Fig. 3, Supplementary Table 10). Our

results show a high risk for porbeagle sharks and white sharks from longline fishing across broad regions, and highlight the need for continued protection—including sufficient coverage by scientific observers on vessels, to underpin accurate data reporting—so that stock rebuilding can continue²⁶. For the northeast Atlantic porbeagle shark, this rebuilding is estimated to take a further 15–30 years to reach sustainable levels even if fishing mortality is reduced to zero¹⁸.

Decreasing the grid-cell size in spatial analyses can lead to concomitant decreases in the estimates of percentages of spatial overlaps^{19,20}, which could potentially affect the patterns of species risk exposure that we found. However, a grid-cell size analysis showed that the patterns of species occurrence within the high- or low-risk zones remained

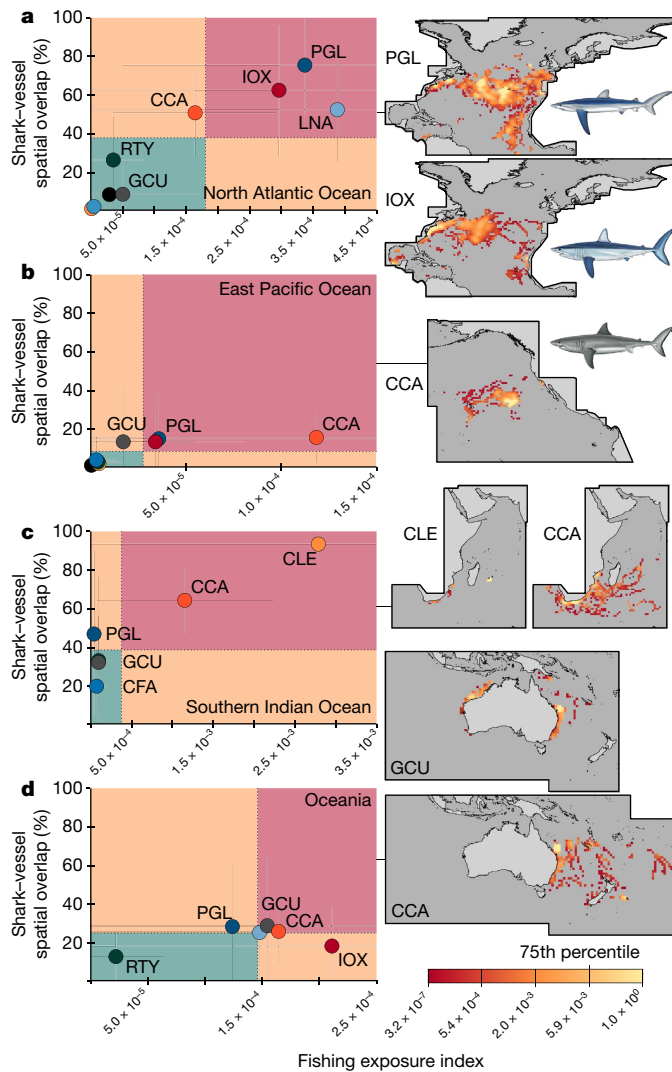


Fig. 3 | Estimated exposure risk of sharks to capture by longline fishing activity. a–d, Plots (left) showing the spatial overlap of sharks and longline fishing effort against species mean monthly FEI indicate species that are subject to high overlap and FEI (higher-risk red zone on plot denotes a higher than average overlap and FEI) and those with lower overlap and FEI (lower-risk green zone denotes a lower than average overlap and FEI) for the North Atlantic Ocean (a), eastern Pacific Ocean (b) and southern Indian Ocean (c), and for the Oceania region (d). Lines separating the coloured zones are fixed at the average values of spatial overlap (y axis) and FEI (x axis) for all species combined. For each ocean, the amount of fishing effort to which individual shark species were exposed (mean FEI; see Methods) is given in the right panel. CCA, *C. carcharias*; CFA, *C. falciformis*; CLE, *C. leucas*; GCU, *G. cuvier*; IOX, *I. oxyrinchus*; LNA, *L. nasus*; PGL, *P. glauca*; RTY, *R. typus*. Error bars denote ± 1 s.d. of the mean.

consistent, irrespective of the spatial scale at which they were observed (Extended Data Fig. 4) or the subset of tracking years that were analysed (Extended Data Figs. 8, 9, see ‘Supplementary results and discussion, section 2.4’ in the Supplementary Information).

Temporal variation in risk

The highest levels of exposure risk of sharks to longline fisheries were not constant through time, but instead varied seasonally as space use by sharks and fishing vessels shifted in relation to each other (Fig. 4, Extended Data Fig. 10). Overall, for species with sufficient data (Fig. 4) the mean monthly overlap of species space use with fishing effort combined with mean FEI showed that sharks spent 4–6 months per year in the lowest-risk zone and 2–6 months in the highest-risk zone, with

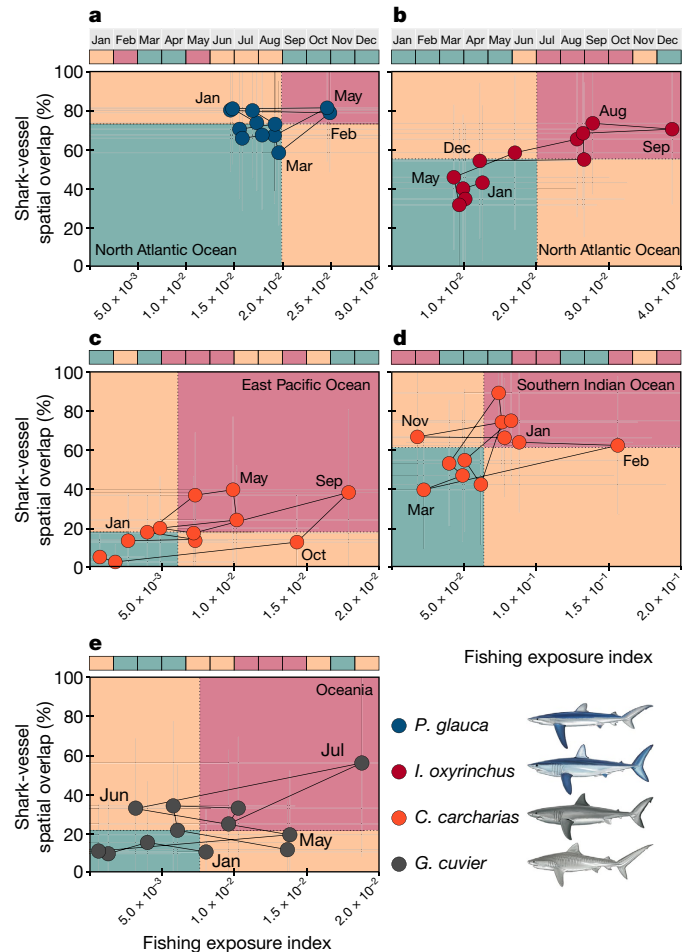


Fig. 4 | Temporal changes in the exposure risk to sharks of longline fishing. a–e, Monthly mean spatial overlap of sharks and longline fishing effort versus monthly mean FEI for all individuals of that species for the four most data-rich species in a relative year: blue sharks (a), shortfin mako sharks (b), white sharks (c, d) and tiger sharks (e). Lines separating the coloured zones are fixed at the respective individual-species average values of spatial overlap (y axis) and FEI (x axis) in a relative year. Horizontal bars denote months in zones with different fishing-exposure risks (red, highest risk; green, lowest risk). Error bars denote ± 1 s.d. of the mean.

differing patterns of changing risk from fishing evident across species (Fig. 4). For example, the highest risk for white sharks in the southwest Indian Ocean and blue sharks in the North Atlantic Ocean occurred at discrete times in the year. For white sharks in the Indian Ocean, this pattern arises from long-range seasonal movements (that take place in December to February, June, July, and October) into annually persistent areas with high mean FEI. For blue sharks, the pattern appears to be driven by sharks and longline vessels co-occurring maximally in boreal winter and summer: lower exposure risk occurs during boreal spring and autumn, as sharks migrate north before returning south⁵. Longline fisheries also make this seasonal south–north–south movement, but lag behind movements of blue sharks (and thus exhibit lower mean overlap and FEI during these times) (Extended Data Fig. 10a–d). Similarly, annual risk patterns of white sharks in the eastern Pacific and tiger sharks from around Australia were driven by migratory behaviour, with the highest risk occurring for three consecutive months in boreal (for white sharks) and austral (for tiger sharks) spring as sharks arrive in areas with higher-than-average exposure to longline-fishing effort (Fig. 4c, e). By contrast, shortfin mako sharks in the North Atlantic Ocean were exposed to high mean overlap (about 60%) and high mean FEI continually through the boreal summer and autumn (July to October), principally owing to their occupation of a space-use

hotspot that is located where the Gulf Stream and Labrador Current converge, which results in persistent high overlap with high levels of longline-fishing effort (Fig. 4b, Extended Data Fig. 10e–h). Tracking of shortfin mako sharks and vessels indicates that fishery-induced mortality within this hotspot is therefore likely to be high. This was confirmed by the high overall return rate of satellite tags (19.3%) attached to shortfin mako sharks in the Atlantic Ocean ($n = 119$ tags; tracking duration: mean \pm s.d., 161.5 ± 156.9 days; median, 109 days), which were returned to us after sharks were captured by longline fleets in the Atlantic Ocean during the study. To our knowledge, this is the highest species-specific return rate for sharks that has yet been recorded in an ocean-scale (as opposed to a regional-scale) study^{27,28} (Fig. 2c, Supplementary Table 13, see ‘Supplementary results and discussion, section 2.6’ in the Supplementary Information).

Discussion

Our results show that globally important habitat areas for threatened pelagic sharks overlap considerably with industrial fishing activity, in both space and time. Given the high levels of fishing effort in hotspots of space use of many species for substantial portions of the year, and the very few tracked hotspots that are free from exploitation, our study reveals that the exposure risk of sharks to fisheries in the high seas is spatially extensive—for some species, this exposure risk stretches nearly across their entire ocean-scale population ranges. Overall, the patterns that we observed suggest a future in which sharks experience only limited spatial refuge from industrial longline-fishing effort, which is currently centred on ecologically important hotspots of space use for oceanic sharks. Our distribution maps are a first, but essential, underpinning for a conservation blueprint for pelagic sharks in the high seas. Our study highlights the scale of the overlap between fishing effort and hotspots of space use by sharks, and argues for more-effective and timely monitoring, reporting and management of pelagic sharks as a result. To enhance the recovery of vulnerable species, one solution is the designation of large-scale marine protected areas²⁹ around ecologically important space-use hotspots of pelagic sharks²⁴—notwithstanding the need for more-complete reporting of catch data, with enforcement to support stricter conventional management bycatch prohibitions, quotas or minimum sizes^{5,16}. This study also outlines shark space-use hotspot locations at which AIS-monitored fishing effort appears at present to be relatively low; these locations are ones in which shark conservation could be maximized, while minimizing the effect on fishing activity that is not directed at sharks (‘Supplementary results and discussion, sections 2.6, 2.7’ in the Supplementary Information). Although it would be challenging to develop a legally binding treaty for managing high-seas fauna²¹, burgeoning technology for global surveillance and enforcement now offers additional options for a step change in ocean management^{6,30}.

Satellite monitoring of marine megafauna^{1,5,11,31}, oceanographic features (eddies and fronts)^{6,24} and the distribution of global fishing vessels^{19,20} could provide signals of shifting space use by wide-ranging sharks and other marine megafauna owing to environmental changes, which—in turn—could inform the designation of new temporary time–area closures to industrial fishing⁶ and the tracking of fishers’ displacement activities²¹. The potential of near-real-time, synoptic measurements of marine megafauna, fishing activity and the marine environment (particularly given the remoteness and vast extent of the high seas) suggests technology-led conservation measures will be crucial tools for reversing the observed declines in iconic ocean predators³ such as pelagic sharks^{12–14,30}. In the future, conservation technology could develop towards the incorporation of adaptive management strategies^{6,30} that are actionable in real time to assess risks in the overlap between fishing vessels and sharks across the global ocean.

Online content

Any methods, additional references, Nature Research reporting summaries, source data, extended data, supplementary information, acknowledgements, peer review information; details of author contributions and competing interests; and

statements of data and code availability are available at <https://doi.org/10.1038/s41586-019-1444-4>.

Received: 4 October 2018; Accepted: 10 July 2019;

Published online: 24 July 2019

- Hays, G. C. et al. Key questions in marine megafauna movement ecology. *Trends Ecol. Evol.* **31**, 463–475 (2016).
- Lewison, R. L. et al. Global patterns of marine mammal, seabird, and sea turtle bycatch reveal taxa-specific and cumulative megafauna hotspots. *Proc. Natl Acad. Sci. USA* **111**, 5271–5276 (2014).
- McCauley, D. J. et al. Marine defaunation: animal loss in the global ocean. *Science* **347**, 1255641 (2015).
- Worm, B., Sandow, M., Oschlies, A., Lotze, H. K. & Myers, R. A. Global patterns of predator diversity in the open oceans. *Science* **309**, 1365–1369 (2005).
- Queiroz, N. et al. Ocean-wide tracking of pelagic sharks reveals extent of overlap with longline fishing hotspots. *Proc. Natl Acad. Sci. USA* **113**, 1582–1587 (2016).
- Scales, K. L. et al. Fisheries bycatch risk to marine megafauna is intensified in Lagrangian coherent structures. *Proc. Natl Acad. Sci. USA* **115**, 7362–7367 (2018).
- O’Connor, S., Ono, R. & Clarkson, C. Pelagic fishing at 42,000 years before the present and the maritime skills of modern humans. *Science* **334**, 1117–1121 (2011).
- Tickler, D., Meeuwij, J.J., Palomares, M.-L., Pauly, D., Zeller, D. Far from home: distance patterns of global fishing fleets. *Sci. Adv.* **4**, eaar3279 (2018).
- Lea, J. S. E. et al. Repeated, long-distance migrations by a philopatric predator targeting highly contrasting ecosystems. *Sci. Rep.* **5**, 11202 (2015).
- Guzman, H. M., Comez, C. G., Hearn, A. & Eckert, S. A. Longest recorded trans-Pacific migration of a whale shark (*Rhincodon typus*). *Mar. Biodivers. Rec.* **11**, 8 (2018).
- Block, B. A. et al. Tracking apex marine predator movements in a dynamic ocean. *Nature* **475**, 86–90 (2011).
- Worm, B. et al. Global catches, exploitation rates, and rebuilding options for sharks. *Mar. Policy* **40**, 194–204 (2013).
- Baum, J. K. et al. Collapse and conservation of shark populations in the Northwest Atlantic. *Science* **299**, 389–392 (2003).
- Ferretti, F., Worm, B., Britten, G. L., Heithaus, M. R. & Lotze, H. K. Patterns and ecosystem consequences of shark declines in the ocean. *Ecol. Lett.* **13**, 1055–1071 (2010).
- Oliver, S., Braccini, M., Newman, S. J. & Harvey, E. S. Global patterns in the bycatch of sharks and rays. *Mar. Policy* **54**, 86–97 (2015).
- Campana, S. E. Transboundary movements, unmonitored fishing mortality, and ineffective international fisheries management pose risks for pelagic sharks in the Northwest Atlantic. *Can. J. Fish. Aquat. Sci.* **73**, 1599–1607 (2016).
- International Commission for the Conservation of Atlantic Tunas (ICCAT). *Report of the 2017 ICCAT Shortfin Mako Assessment Meeting (Madrid, Spain)*. <https://www.iccat.int/en/assess.html> (2017).
- International Commission for the Conservation of Atlantic Tunas. *Report of the Standing Committee on Research and Statistics (SCRS)*. doc. no. PLE 104/2017 <https://www.iccat.int/en/scrs.html> (2017).
- Kroodsma, D.A. et al. Tracking the global footprint of fisheries. *Science* **359**, 904–908 (2018).
- Kroodsma, D.A. et al. Response to Comment on “Tracking the global footprint of fisheries”. *Science* **361**, eaat7789 (2018).
- McCauley, D. J. et al. Ending hide and seek at sea. *Science* **351**, 1148–1150 (2016).
- Shepperson, J. L. et al. A comparison of VMS and AIS data: the effect of data coverage and vessel position recording frequency on estimates of fishing footprints. *ICES J. Mar. Sci.* **75**, 988–998 (2018).
- Sala, E. et al. The economics of fishing the high seas. *Sci. Adv.* **4**, eaat2504 (2018).
- Scales, K. L. et al. On the front line: frontal zones as priority at-sea conservation areas for mobile marine vertebrates. *J. Appl. Ecol.* **51**, 1575–1583 (2014).
- Fields, A. T. et al. Species composition of the international shark fin trade assessed through a retail-market survey in Hong Kong. *Conserv. Biol.* **32**, 376–389 (2018).
- Curtis, T. H. et al. Seasonal distribution and historic trends in abundance of white sharks, *Carcharodon carcharias*, in the western North Atlantic Ocean. *PLoS ONE* **9**, e99240 (2014).
- Kohler, N. E. & Turner, P. A. Shark tagging: a review of conventional methods and studies. *Environ. Biol. Fishes* **60**, 191–224 (2001).
- Byrne, M. E. et al. Satellite telemetry reveals higher fishing mortality rates than previously estimated, suggesting overfishing of an apex marine predator. *Proc. R. Soc. Lond. B* **284**, 20170658 (2017).
- O’Leary, B. C. et al. Addressing criticisms of large-scale marine protected areas. *Bioscience* **68**, 359–370 (2018).
- Hays, G. C. et al. Translating marine animal tracking data into conservation policy and management. *Trends Ecol. Evol.* **34**, 459–473 (2019).
- Sequeira, A. M. M. et al. Convergence of marine megafauna movement patterns in coastal and open oceans. *Proc. Natl Acad. Sci. USA* **115**, 3072–3077 (2018).

Publisher’s note: Springer Nature remains neutral with regard to jurisdictional claims in published maps and institutional affiliations.

© The Author(s), under exclusive licence to Springer Nature Limited 2019

Nuno Queiroz^{1,2}, Nicolas E. Humphries², Ana Couto¹, Marisa Vedor^{1,3}, Ivo da Costa¹, Ana M. M. Sequeira^{4,5}, Gonzalo Mucientes¹, António M. Santos^{1,3}, Francisco J. Abascal⁶, Debra L. Abercrombie⁷, Katya Abrantes⁸, David Acuña-Marrero⁹, André S. Afonso^{10,11}, Pedro Afonso^{12,13,14}, Darrell Anders¹⁵, Gonzalo Araujo¹⁶, Randall Arauz^{17,18,19}, Pascal Bach²⁰, Adam Barnett⁸, Diego Bernal²¹, Michael L. Berumen²², Sandra Bessudo Lion^{19,23}, Natalia P. A. Bezerra¹⁰, Antonin V. Blaison²⁰, Barbara A. Block²⁴, Mark E. Bond²⁵, Ramón Bonfil²⁶, Russell W. Bradford²⁷, Camrin D. Braun²⁸, Edward J. Brooks²⁹, Annabelle Brooks^{29,30}, Judith Brown³¹, Barry D. Bruce²⁷, Michael E. Byrne^{32,33}, Steven E. Campana³⁴, Aaron B. Carlisle³⁵, Demian D. Chapman²⁵, Taylor K. Chapple²⁴, John Chisholm³⁶, Christopher R. Clarke³⁷, Eric G. Clua³⁸, Jesse E. M. Cochran²², Estelle C. Crochelet^{39,40}, Laurent Dagorn²⁰, Ryan Daly^{41,42}, Daniel Devia Cortés⁴³, Thomas K. Doyle^{44,45}, Michael Drew⁴⁶, Clinton A. J. Duffy⁴⁷, Thor Erikson⁴⁸, Eduardo Espinoza^{19,49}, Luciana C. Ferreira⁵⁰, Francesco Ferretti²⁴, John D. Filmlalter^{20,42}, G. Chris Fischer⁵¹, Richard Fitzpatrick⁸, Jorge Fontes^{12,13,14}, Fabien Forget²⁰, Mark Fowler⁵², Malcolm P. Francis⁵³, Austin J. Gallagher^{54,55}, Enrico Gennari^{42,56,57}, Simon D. Goldsworthy⁵⁸, Matthew J. Gollock⁵⁹, Jonathan R. Green⁶⁰, Johan A. Gustafson⁶¹, Tristan L. Guttridge⁶², Hector M. Guzman⁶³, Neil Hammerschlag^{55,64}, Luke Harman⁴⁴, Fábio H. V. Hazin¹⁰, Matthew Heard⁴⁶, Alex R. Hearn^{19,65,66}, John C. Holdsworth⁶⁷, Bonnie J. Holmes⁶⁸, Lucy A. Howey⁶⁹, Mauricio Hoyos^{19,70}, Robert E. Hueter⁷¹, Nigel E. Hussey⁷², Charlie Huvener⁴⁶, Dylan T. Irion⁷³, David M. P. Jacoby⁷⁴, Oliver J. D. Jewell^{75,76}, Ryan Johnson⁷⁷, Lance K. B. Jordan⁶⁹, Salvador J. Jorgensen⁷⁸, Warren Joyce⁵², Clare A. Keating Daly⁴¹, James T. Ketchum^{19,70}, A. Peter Klimley^{19,79}, Alison A. Kock^{42,80,81,82}, Pieter Koen⁸³, Felipe Ladino²³, Fernanda O. Lana⁸⁴, James S. E. Lea^{37,85}, Fiona Llewellyn⁵⁹, Warrick S. Lyon⁵³, Anna MacDonnell⁵², Bruno C. L. Macena^{10,13}, Heather Marshall^{21,86}, Jaime D. McAllister⁸⁷, Rory McAuley^{88,89}, Michael A. Meyer¹⁵, John J. Morris⁷¹, Emily R. Nelson⁵⁵, Yannis P. Papastamatiou²⁵, Toby A. Patterson²⁷, Cesar Peñaherrera-Alpama^{19,90}, Julian G. Pepperbee⁹¹, Simon J. Pierce⁹², Francois Poisson²⁰, Lina Maria Quintero²³, Andrew J. Richardson⁹³, Paul J. Rogers⁵⁸, Christoph A. Rohner⁹², David R. L. Rowat⁹⁴, Melita Samoilys⁹⁵, Jayson M. Semmens⁸⁷, Marcus Sheaves⁸, George Shillinger^{19,24,96}, Mahmood Shivji³², Sarika Singh¹⁵, Gregory B. Skomal³⁶, Malcolm J. Smale⁹⁷, Laurence B. Snyders¹⁵, German Soler^{19,23,87}, Marc Soria²⁰, Kilian M. Stehfest⁸⁷, John D. Stevens²⁷, Simon R. Thorrold⁹⁸, Mariana T. Tolotti²⁰, Alison Towner^{57,76}, Paulo Travassos¹⁰, John P. Tyminski⁷¹, Frederic Vandepierre^{12,13,14}, Jeremy J. Vaudo³², Yuuki Y. Watanabe^{99,100}, Sam B. Weber¹⁰¹, Bradley M. Wetherbee^{32,102}, Timothy D. White²⁴, Sean Williams²⁹, Patricia M. Zárte^{19,103}, Robert Harcourt¹⁰⁴, Graeme C. Hays¹⁰⁵, Mark G. Meekan³⁰, Michele Thums⁵⁰, Xabier Irigoien^{106,107}, Victor M. Eguiluz¹⁰⁸, Carlos M. Duarte²², Lara L. Sousa^{2,109}, Samantha J. Simpson^{2,110}, Emily J. Southall² & David W. Sims^{2,110,111*}

¹Centro de Investigação em Biodiversidade e Recursos Genéticos/Research Network in Biodiversity and Evolutionary Biology, Campus Agrário de Vairão, Universidade do Porto, Vairão, Portugal. ²Marine Biological Association of the United Kingdom, Plymouth, UK. ³Departamento de Biologia, Faculdade de Ciências da Universidade do Porto, Porto, Portugal. ⁴UWA Oceans Institute, Indian Ocean Marine Research Centre, University of Western Australia, Crawley, Western Australia, Australia. ⁵School of Biological Sciences, University of Western Australia, Crawley, Western Australia, Australia. ⁶Spanish Institute of Oceanography, Santa Cruz de Tenerife, Spain. ⁷Abercrombie and Fish, Port Jefferson Station, Jefferson, NY, USA. ⁸Marine Biology and Aquaculture Unit, College of Science and Engineering, James Cook University, Cairns, Queensland, Australia. ⁹School of Natural and Computational Sciences, Massey University, Palmerston North, New Zealand. ¹⁰Universidade Federal Rural de Pernambuco (UFRPE), Departamento de Pesca e Aquicultura, Recife, Brazil. ¹¹MARE, Marine and Environmental Sciences Centre, Instituto Politécnico de Leiria, Peniche, Portugal. ¹²MARE, Laboratório Marítimo da Guia, Faculdade de Ciências da Universidade de Lisboa, Cascais, Portugal. ¹³Institute of Marine Research (IMAR), Departamento de Oceanografia e Pescas, Universidade dos Açores, Horta, Portugal. ¹⁴Oceanos - Departamento de Oceanografia e Pescas, Universidade dos Açores, Horta, Portugal. ¹⁵Department of Environmental Affairs, Oceans and Coasts Research, Cape Town, South Africa. ¹⁶Large Marine Vertebrates Research Institute Philippines, Jagna, Philippines. ¹⁷Fins Attached Marine Research and Conservation, Colorado Springs, CO, USA. ¹⁸Programa Restauración de Tortugas Marinas PRETOMA, San José, Costa Rica. ¹⁹MigraMar, Olema, CA, USA. ²⁰Institut de Recherche pour le Développement, UMR MARBEC (IRD, Ifremer, Université de Montpellier, CNRS), Sète, France. ²¹Biology Department, University of Massachusetts Dartmouth, Dartmouth, MA, USA. ²²Red Sea Research Center, Division of Biological and Environmental Science and Engineering, King Abdullah University of Science and Technology, Thuwal, Saudi Arabia. ²³Fundación Malpelo y Otros Ecosistemas Marinos, Bogota, Colombia. ²⁴Hopkins Marine Station of Stanford University, Pacific Grove, CA, USA. ²⁵Department of Biological Sciences, Florida International University, North Miami, FL, USA. ²⁶Océanos Vivos, Mexico City, Mexico. ²⁷CSIRO Oceans and Atmosphere, Hobart, Tasmania, Australia. ²⁸Massachusetts Institute of Technology–Woods Hole Oceanographic

Institution Joint Program in Oceanography/Applied Ocean Science and Engineering, Cambridge, MA, USA. ²⁹Shark Research and Conservation Program, Cape Eleuthera Institute, Eleuthera, Bahamas. ³⁰University of Exeter, Exeter, UK. ³¹South Atlantic Environmental Research Institute, Stanley, Falkland Islands. ³²Department of Biological Sciences, The Guy Harvey Research Institute, Nova Southeastern University, Dania Beach, FL, USA. ³³School of Natural Resources, University of Missouri, Columbia, MO, USA. ³⁴Life and Environmental Sciences, University of Iceland, Reykjavik, Iceland. ³⁵School of Marine Science and Policy, University of Delaware, Lewes, DE, USA. ³⁶Massachusetts Division of Marine Fisheries, New Bedford, MA, USA. ³⁷Marine Research Facility, Jeddah, Saudi Arabia. ³⁸PSL, Labex CORAIL, CRIObE USR3278 EPHE-CNRS-UPVD, Papetō'ai, French Polynesia. ³⁹Agence de Recherche pour la Biodiversité à la Réunion (ARBRE), Saint-Denis, Réunion, Marseille, France. ⁴⁰Institut de Recherche pour le Développement, UMR 228 ESPACE-DEV, Saint-Denis, Réunion, Marseille, France. ⁴¹Save Our Seas Foundation–D'Arros Research Centre (SOSF–DRC), Geneva, Switzerland. ⁴²South African Institute for Aquatic Biodiversity (SAIAB), Grahamstown, South Africa. ⁴³Department of Fisheries Evaluation, Fisheries Research Division, Instituto de Fomento Pesquero (IFOP), Valparaíso, Chile. ⁴⁴School of Biological, Earth and Environmental Sciences, University College Cork, Cork, Ireland. ⁴⁵MaREI Centre, Environmental Research Institute, University College Cork, Cork, Ireland. ⁴⁶College of Science and Engineering, Flinders University, Adelaide, South Australia, Australia. ⁴⁷Department of Conservation, Auckland, New Zealand. ⁴⁸Geological Sciences, South African Institute for Aquatic Biodiversity (SAIAB), Durban, South Africa. ⁴⁹Dirección Parque Nacional Galapagos, Puerto Ayora, Ecuador. ⁵⁰Australian Institute of Marine Science, Indian Ocean Marine Research Centre (IOWA), Crawley, Western Australia, Australia. ⁵¹OCEARCH, Park City, UT, USA. ⁵²Bedford Institute of Oceanography, Dartmouth, Nova Scotia, Canada. ⁵³National Institute of Water and Atmospheric Research, Wellington, New Zealand. ⁵⁴Beneath the Waves, Herndon, VA, USA. ⁵⁵Rosenstiel School of Marine and Atmospheric Science, University of Miami, Miami, FL, USA. ⁵⁶Oceans Research, Mossel Bay, South Africa. ⁵⁷Department of Ichthyology and Fisheries Science, Rhodes University, Grahamstown, South Africa. ⁵⁸SARDI Aquatic Sciences, Adelaide, South Australia, Australia. ⁵⁹Zoological Society of London, London, UK. ⁶⁰Galapagos Whale Shark Project, Puerto Ayora, Galapagos Islands, Ecuador. ⁶¹Griffith Centre for Coastal Management, Griffith University School of Engineering, Griffith University, Gold Coast, Queensland, Australia. ⁶²Bimini Biological Field Station, South Bimini, Bahamas. ⁶³Smithsonian Tropical Research Institute, Panama City, Panama. ⁶⁴Leonard and Jayne Abess Center for Ecosystem Science and Policy, University of Miami, Coral Gables, FL, USA. ⁶⁵Galapagos Science Center, San Cristobal, Ecuador. ⁶⁶Universidad San Francisco de Quito, Quito, Ecuador. ⁶⁷Blue Water Marine Research, Tutukaka, New Zealand. ⁶⁸University of Queensland, Brisbane, Queensland, Australia. ⁶⁹Microwave Telemetry, Columbia, MD, USA. ⁷⁰Pelagios-Kakunja, La Paz, Mexico. ⁷¹Mote Marine Laboratory, Center for Shark Research, Sarasota, FL, USA. ⁷²Biological Sciences, University of Windsor, Windsor, Ontario, Canada. ⁷³Cape Research and Diver Development, Simon's Town, South Africa. ⁷⁴Institute of Zoology, Zoological Society of London, London, UK. ⁷⁵Centre for Sustainable Aquatic Ecosystems, Harry Butler Institute, Murdoch University, Perth, Western Australia, Australia. ⁷⁶Dyer Island Conservation Trust, Kleinbaai, South Africa. ⁷⁷Blue Wilderness Research Unit, Scotland, South Africa. ⁷⁸Monterey Bay Aquarium, Monterey, CA, USA. ⁷⁹University of California Davis, Davis, CA, USA. ⁸⁰Cape Research Centre, South African National Parks, Steenberg, South Africa. ⁸¹Shark Spotters, Fish Hoek, South Africa. ⁸²Institute for Communities and Wildlife in Africa, Department of Biological Sciences, University of Cape Town, Cape Town, South Africa. ⁸³Veterinary Services, Western Cape Department of Agriculture, Elsenburg, South Africa. ⁸⁴Departamento de Biologia Marinha, Universidade Federal Fluminense (UFF), Niterói, Brazil. ⁸⁵Department of Zoology, University of Cambridge, Cambridge, UK. ⁸⁶Atlantic White Shark Conservancy, Chatham, MA, USA. ⁸⁷Fisheries and Aquaculture Centre, Institute for Marine and Antarctic Studies, University of Tasmania, Hobart, Tasmania, Australia. ⁸⁸Department of Fisheries, Government of Western Australia, Perth, Western Australia, Australia. ⁸⁹Minderoo Foundation, Flourishing Oceans Initiative, Perth, Western Australia, Australia. ⁹⁰Pontificia Universidad Católica del Ecuador Sede Manabi, Portoviejo, Ecuador. ⁹¹Pepperell Research and Consulting, Noosa, Queensland, Australia. ⁹²Marine Megafauna Foundation, Truckee, CA, USA. ⁹³Conservation and Fisheries Department, Ascension Island Government, Georgetown, Ascension Island, UK. ⁹⁴Marine Conservation Society Seychelles, Victoria, Seychelles. ⁹⁵CORDIO, Mombasa, Kenya. ⁹⁶Upwell, Monterey, CA, USA. ⁹⁷Department of Zoology and Institute for Coastal and Marine Research, Nelson Mandela University, Port Elizabeth, South Africa. ⁹⁸Biology Department, Woods Hole Oceanographic Institution, Woods Hole, MA, USA. ⁹⁹National Institute of Polar Research, Tachikawa, Tokyo, Japan. ¹⁰⁰Department of Polar Science, SOKENDAI (The Graduate University for Advanced Studies), Tachikawa, Tokyo, Japan. ¹⁰¹Centre for Ecology and Conservation, University of Exeter, Penryn, UK. ¹⁰²Department of Biological Sciences, University of Rhode Island, Kingston, RI, USA. ¹⁰³Department of Oceanography and Environment, Fisheries Research Division, Instituto de Fomento Pesquero (IFOP), Valparaíso, Chile. ¹⁰⁴Department of Biological Sciences, Macquarie University, Sydney, New South Wales, Australia. ¹⁰⁵School of Life and Environmental Sciences, Deakin University, Geelong, Victoria, Australia. ¹⁰⁶AZTI - Marine Research, Pasaia, Spain. ¹⁰⁷IKERBASQUE, Basque Foundation for Science, Bilbao, Spain. ¹⁰⁸Instituto de Física Interdisciplinar y Sistemas Complejos, Consejo Superior de Investigaciones Científicas, University of the Balearic Islands, Palma de Mallorca, Spain. ¹⁰⁹Wildlife Conservation Research Unit, Department of Zoology, University of Oxford, Tubney, UK. ¹¹⁰Ocean and Earth Science, National Oceanography Centre Southampton, University of Southampton, Southampton, UK. ¹¹¹Centre for Biological Sciences, University of Southampton, Southampton, UK. *e-mail: dws@mba.ac.uk

METHODS

No statistical methods were used to predetermine sample size. The experiments were not randomized and investigators were not blinded to allocation during experiments and outcome assessment.

Study animals and tagging. From 2002 to 2017, we tagged 1,804 pelagic sharks with satellite transmitters at multiple tagging sites in the Atlantic Ocean, Indian Ocean and Pacific Ocean (Extended Data Fig. 1), including 649 in the North Atlantic Ocean, 588 in the eastern Pacific Ocean, 151 in Oceania and 153 in the southwest Indian Ocean: 60% of deployments occurred between 2010 and 2017 (Extended Data Fig. 1, Supplementary Tables 3–5). The number of tagged individuals varied among species, and ranged from 1 to 280. Two types of satellite-transmitter tag (position-only advanced research and global observation satellite (ARGOS) transmitter and pop-off satellite archival transmitter (PSAT)) were used. Sharks were captured with baited hooks (longlines, rod-and-line angling or with handlines), in purse seine during commercial fishing operations, or tagged free-swimming in the water. Tags were attached to the first dorsal fin or in the dorsal musculature. All animal handling procedures were approved by institutional ethical review committees and completed by trained personnel (see Supplementary Information for details). Data were provided by the data owners to the senior author and quality-checked before archiving in a database. Poor-quality data were reported for 123 tags (72 ARGOS and 51 PSAT), owing to (for example) early tag failure, premature tag pop-off or a high percentage of locations estimated with high spatial error (for example, raw computed geolocations over land). All of these resulted in poor state-space model fits, which led to short or unreliable track reconstructions. Analyses were therefore restricted to the remaining 1,681 tracks from 1,066 ARGOS and 615 PSAT tags on sharks from 23 species, ranging in total duration per species from 20 to 57,037 days with a median of 4.1 years total track time per species (Supplementary Table 3). The number of sharks tracked within each region is given in Supplementary Table 14.

Track processing. Movements of PSAT-tagged sharks were estimated using either satellite-released data from each tag or from archival data after the tags were physically recovered. Data were provided as: (i) raw shark positions that were previously reconstructed using software provided by the tag manufacturers (for example, Wildlife Computers or Microwave Telemetry), in which daily maximal rate-of-change in light intensity was used to estimate local time of midnight or midday for longitude calculations, and day-length estimation for determining latitude^{32,33}, or (ii) filtered positions in which a state-space model (SSM) (unscented Kalman filter with sea-surface temperature, UKFSST)³⁴ had been applied to correct the raw geolocation estimates and obtain the most-probable track. In the first case, raw positions were corrected using the UKFSST SSM (UKFSST R package) in addition to a bathymetric correction applied to the initial Kalman position estimates (analyzepsat R add-on). A daily time-series of locations was estimated using a continuous-time correlated random walk (CTCRW) Kalman filter³⁵ (crawl R package). UKFSST geolocations were parameterized with s.d. constants, which produces the smallest mean deviation from concurrent ARGOS positions³⁶. In the latter case, the CTCRW SSM was applied to produce regular time-series.

For ARGOS transmitter tags, data were provided as raw ARGOS (Doppler frequency shift) position estimates. Location class Z data—assigned for a failed attempt at obtaining a position—were discarded from the dataset. The remaining raw position estimates (location classes 3, 2, 1, 0, A and B) were analysed point-to-point with a speed filter of 3 m s^{-1} to remove outlier locations. Subsequently, the CTCRW SSM was applied to each individual track, which produced a single position estimate per day using model parameters implemented in the crawl R package³⁵.

Shark tracking data from the Tagging of Pacific Predators (TOPP) program were downloaded from the Animal Tracking Network hosted by the Integrated Ocean Observing System (<https://ioos.noaa.gov/project/atn/>, downloaded September 2017). Both ARGOS and light-based geolocation data in the Animal Tracking Network had already been filtered with a Bayesian-based SSM³⁷. In brief, the SSM was fitted to each track individually, using the WinBUGS software that conducts Bayesian statistical analyses using Markov chain Monte Carlo sampling³⁸. For each track, two Markov chain Monte Carlo chains each of length 10,000 were run and a sample of 2,000 from the joint posterior probability distribution was obtained by discarding the first 5,000 iterations and retaining every 5th of the remaining iterations. SSM fits were posteriorly inspected for obvious problems (for example, unrealistic movements¹¹). Because two different SSMs were applied to data used in this study, we tested for possible biases in the spatial density analysis (see ‘Spatial density analysis’) by comparing $1^\circ \times 1^\circ$ density grid maps obtained with both UKFSST and Bayesian-based filtered tracks using a subset of 83 ARGOS-linked tracks in the North Atlantic Ocean (blue shark, $n = 27$; shortfin mako shark, $n = 42$; white shark, $n = 3$; and oceanic whitetip shark, $n = 11$). Differences in spatial grid density between the two methods were negligible (Supplementary Fig. 1). Thus, tracks with daily locations were reconstructed for 1,681 individuals, totalling 281,724 tracking days (Supplementary Table 3).

Spatial density analysis. To obtain unbiased estimates of shark spatial density, gaps between consecutive dates in the raw tracking data were interpolated to one position per day. Long temporal gaps without tag-reported location data in a reconstructed track can result in extensive interpolated movements driven by the underlying random walk model rather than the movement pattern of the shark¹¹. Although the frequency of long temporal gaps without data (>20 days) in our dataset was low (Supplementary Table 15), any tracks with gaps without data that exceeded 20 days were nonetheless split into segments before interpolation, thus avoiding the inclusion of unrepresentative interpolated location estimates⁵. Similarly, location estimates derived for periods without data that exceeded 20 days were also discarded from TOPP data¹¹.

To account for biases in spatial location density associated with (i) variable track lengths and (ii) shorter tracks near the tagging location, we broadly followed a previously published basic time weighting procedure¹¹. In this study, each daily location estimate of an individual was weighted by the inverse of the number of all individuals with location estimates for the same relative day of their track:

$$w_{it} = 1/n_t \text{ for } i \in I \quad (1)$$

in which w_{it} is the weight for the t th location estimate of the track of the i th individual, n_t is the number of total individuals with a t th location estimate, and I is the set of individuals of all species. We calculated weights for all individuals, irrespective of species, to estimate the global relative spatial density of pelagic sharks (that is, Fig. 2a). Periods with gaps without data that exceeded 20 days were not included when weighting the locations. To minimize bias in estimates of spatial density patterns when sample sizes were lower, a modified version of a previously published weighting procedure¹¹ was implemented, such that location weights after a threshold day of the relative track were fixed equal to the weight on the day corresponding to the 85th percentile of track lengths. Under this weighting scheme, individual location estimates closer to the tagging location tended to receive a lower weight than later locations as—owing to tag failure—transmissions of satellite locations are more likely earlier in the track of an individual shark. Therefore, longer tracks received a higher total weight than shorter tracks because of the lower number of long tracks and, consequently, the lower value of n_t towards the end of the track. Calculated spatial densities were therefore more representative of the actual distributions, and less affected by tag loss, failure or a spatial bias towards deployment location.

The weights for all individuals (equation (1)) were normalized so that they summed to unity. Therefore, within the study area, all individuals contributed equally to the described global spatial density patterns:

$$D_{it} = \sum_{i \in I} \sum_{t=1}^T w_{it}$$

in which D_{it} is the relative density contribution of the t th location estimate for individual i , and T_i is the number of location estimates for individual i . The relative density contributions for all location estimates for all individuals (D_{it}) were then summed within each grid cell of the study area for each month of a relative year, which gave 12 spatial relative density maps to compare with monthly longline-fishing effort. The mean annual D_{it} per grid cell for a relative year was calculated from the 12 monthly relative densities per grid cell to provide the global relative density of tracked sharks mapped in Fig. 2a. Hammerhead sharks (3 species) and mako sharks (2 species) were analysed as taxa groups: *Sphyrna* spp. and *Isurus* spp., respectively. The spatial coverage of $1^\circ \times 1^\circ$ grid cells occupied by sharks per ocean region was between 53% (eastern Pacific Ocean) and 25% (Oceania) of total grid cells (Supplementary Table 15). Spatial relative densities of locations were also calculated for each of the ten most data-rich species separately at a $1^\circ \times 1^\circ$ grid-cell size (Extended Data Figs. 6, 7). We followed the same procedure as for the all-species spatial density calculation, but instead weighted by the inverse of the number of total individuals of a single species on the same relative day of their track, and with the weights for each species normalized to one.

To examine how the broad spatial distribution of sharks between years may have changed, we re-calculated the relative density contributions for all location estimates for all individuals (D_{it}) together within each of eight consecutive two-year classes starting in 2002 (Extended Data Fig. 8). Each daily location within a class was weighted by the inverse of the number of individuals with location estimates for the same relative day of the two years (for example, 1 January 2012 is the relative day 1 of all tracks in each of two years that were active on that date). Similar to the weighting scheme applied to the main data, periods with gaps without data that exceeded 20 days were not included when weighting the locations. After the 85th percentile of the track length, daily weights were fixed as for the all-species spatial density. Total weights for all individuals within each two-year class were normalized to one. In addition, owing to a mismatch in the years of data availability between sharks and fishing vessels, exposure risk (overlap and FEI) was

re-calculated for the period between 2012 and 2016, which was common to both sharks and longline-fishing vessels (Extended Data Fig. 9). Relative density of all individuals (D_{it}) was re-calculated on the basis of the weighting scheme, considering only individuals with tracks that were within the 2012–2016 period.

Fishing vessel geolocation data. The AIS was developed as a vessel safety and anti-collision system with global coverage, rather than to track fishing vessels for fishery management purposes^{19–23}. However, its global coverage of the locations of many thousands of ships through time enables the analysis of the distribution of fishing effort^{19–23}. Here, fishing-effort (hours of fishing) data, gridded at 0.01° by flag state, and estimated gear type were obtained from Global Fishing Watch (GFW) (available at <https://globalfishingwatch.org/datasets-and-code/fishing-effort/>). GFW used raw AIS vessel tracking data obtained from ORBCOMM via their AIS-enabled satellite constellation (<https://www.orbcomm.com/eu/networks/satellite-ais>) to calculate fishing effort and derive the gridded data, as previously described in detail^{19,20}. In brief, GFW uses two neural network algorithms to categorize different types of fishing gear (for example, drifting longlines or purse seines), in addition to estimating the spatiotemporally resolved locations at which fishing gears were most likely to be deployed by individual vessels^{19,20}. We used the GFW gridded fishing-effort data in the years 2012 to 2016 for all gear types, and for estimated drifting pelagic longlines and purse seines. The GFW gear-type classification algorithms are being continuously refined to correct for acknowledged contamination of some gear types with others in some regions^{19,20} (for example, drifting longlines with bottom-set longlines off New Zealand). For each gear type in this study, we summed the number of hours fishing in a month (expressed as days, in which 24 h of fishing effort = 1 day) within each $1^\circ \times 1^\circ$ grid cell to provide 12 monthly global fishing-effort maps. The mean annual fishing effort per grid cell in a relative year was calculated from the 12 monthly fishing-effort maps. Global distributions of fishing effort for all gear types, longlines and purse seines were mapped separately and overlaid by shark spatial relative density of locations for all individuals (D_{it}) to determine spatial overlap intensity (the fishing effort to which sharks were exposed; see ‘Shark and vessel spatial overlap and effort’). AIS data coverage increased from 2012 to 2016 as more satellite AIS receivers were launched and commenced operation^{19,20}. However, the global spatial distribution of longline-vessel fishing effort was broadly similar across years (Supplementary Fig. 2), and variation in annual maximum fishing effort displayed no increasing trend over time, which indicated that our calculated mean annual fishing effort for 2012–2016 did not overestimate the spatial overlap or fishing effort, but can be considered conservative (Supplementary Fig. 2). To test that the numbers of longline fishing days per grid cell from AIS data were representative of actual fishing effort as measured by the numbers of baited hooks deployed by longline vessels, we correlated fishing days using AIS data from the Atlantic Ocean with International Commission for the Conservation of Atlantic Tunas (ICCAT) observed hook data (downloaded from <https://iccat.int/en/accesingdb.html>). We compared the total number of observed hooks in ICCAT data at a $5^\circ \times 5^\circ$ grid-cell size (the finest spatial resolution for these ICCAT data) with the total number of fishing days in the AIS dataset, also at $5^\circ \times 5^\circ$. To calculate the fishing-effort days from AIS data in each $5^\circ \times 5^\circ$ grid cell, we summed the days in the $1^\circ \times 1^\circ$ cells that fell within each $5^\circ \times 5^\circ$ cell. Data were used from 2015, the most recent year for which we had both ICCAT hook data and comprehensive longline-fishing coverage from AIS data.

Shark and fishing-effort environment modelling. To model shark and fishing vessel distributions in relation to environmental variables, data were extracted from online databases (Supplementary Fig. 3). The environmental variables were selected on the basis of their demonstrated importance in affecting shark occurrence and included: (i) sea water temperature ($^\circ\text{C}$) (abbreviation used in models: sea-surface temperature, SST; temperature at 100 m, TEM_100), which is known to influence the presence of many pelagic shark species^{5,11}; (ii) maximum thermal gradient ($\Delta^\circ\text{C}$ per 100 km) (TGR) influences shark spatial density⁵, and was calculated here on the basis of the SST data and using maximum gradient maps by determining where, for each pixel, a geodetic-distance-corrected maximum thermal gradient was identified; (iii) sea water salinity (in psu) (SAL), an important determinant of habitat use in some sharks^{1,39}; (iv) sea-surface height above geoid (in m) (SSH), which influences shark presence⁵ and catches by fisheries⁶; (v) ocean mixed-layer depth thickness or thermocline depth (in m) (MLD), which affects the foraging behaviour of pelagic sharks⁴⁰; (vi) mass of chlorophyll *a* in sea water (mg m^{-3}) (CHL) as a proxy for productivity, which often characterizes the preferred habitats of sharks^{5,40}; (vii) mole concentration of phytoplankton, expressed as carbon in sea water concentration (mmol m^{-3}) (PHY), as a direct measure of productivity; (viii) net primary production of biomass, expressed as carbon per unit volume in sea water per day ($\text{g m}^{-3} \text{d}^{-1}$) (NPP), which quantifies productivity; and (ix) mole concentration of dissolved molecular oxygen in sea water (mmol m^{-3}) (DO), which can strongly influence shark space use¹. Environmental datasets i–v were downloaded from Copernicus Marine Environment Monitoring Service (CMEMS) Global Ocean Physics Reanalysis product (http://marine.copernicus.eu/services-portfolio/access-to-products/?option=com_csw&view=details

&product_id=GLOBAL_REANALYSIS_PHY_001_025; downloaded November 2017) and datasets vi–ix from CMEMS Global Ocean Biochemistry Hindcast product (http://marine.copernicus.eu/services-portfolio/access-to-products/?option=com_csw&view=details&product_id=GLOBAL_REANALYSIS_BIO_001_029; downloaded November 2017). CMEMS data were available for 2002 to 2014 from the surface to 5,500 m as monthly datasets. Overall averages (2002–2014) were calculated at a $1^\circ \times 1^\circ$ grid-cell resolution for surface and 100-m depth layers (with the exception of SSH and MLD) (Supplementary Fig. 3). Most of these variables and interactions are also considered important for explaining fishing patterns^{5,6}.

We developed and compared a set of generalized additive models (GAMs) with a Gaussian family and an identity link, using the log-transformed relative density of locations of all individual sharks (D_{it}) as the response variable. We used the relative density of sharks rather than presence and absence data, because our main aim was to highlight the areas in which the highest overlap with fishing effort might occur. Because we were interested in identifying areas (grid cells) with the highest overlap, and understanding how general environmental variables might influence shark density in specific locations, we considered the relative density for all 23 shark species combined without considering random effects per species. All environmental variables were standardized (mean-centred and divided by the s.d.) and collinearity was checked before inclusion in the models. Highly skewed environmental variables were logged before standardization: this included most predictors at the surface (except for SAL and SSH), as well as NPP (for sharks only) and TGR at 100 m (TGR_100). All possible combinations of 16 variables were not undertaken, owing to collinearity. Rather, we focused on testing ecologically relevant hypotheses. A description of the general hypothesis tested with each model included in the model set is given in Supplementary Table 7. It was necessary to include models with a reduced number of variables because some variables were collinear, and those variables were included in other models. Because sharks respond to surface and subsurface thermal gradients (which often support higher biological productivity)^{5,6,11,40}, we tested for interactions between MLD and SST, CHL and MLD at 100 m (MLD_100), CHL at 100 m (CHL_100) and TEM at 100 m (TEM_100), MLD and TGR at the surface, MLD and CHL_100, CHL_100 and TEM_100, and between SAL and TEM_100.

A GAM with a Tweedie distribution and log-link function provided the best modelling approach for the fishing effort data (including zeros in grid cells), as this distribution includes a family of probability distributions including normal, gamma, Poisson and compound Poisson–gamma. We considered two response variables separately: fishing effort (days of fishing per grid cell) of all AIS-equipped fishing vessels, and fishing effort of AIS-equipped longline-fishing vessels only. We did not consider presence and absence data, because our aim was to understand how environment influenced variations in fishing effort. In our model set, we included different combinations of a total of the same 16 explanatory environmental variables used for shark density modelling (Supplementary Table 7), and also a null (all terms equal to zero), intercept-only model. The dimension basis for all terms was limited to 5 (that is, $k = 5$) to assist controlling for overfitting⁴¹. We then used the Akaike’s information criterion (AIC)⁴² to compare the models in the model set for all sharks and fishing vessels. We assessed the relative strength of evidence for each model using the weights of AIC, and the goodness-of-fit of each model by calculating the percentage of deviance explained (%DE). All models were implemented in R using the mgcv package⁴³.

Shark and vessel spatial overlap and effort. The spatial overlap (in per cent) between an individual tracked shark and fishing effort was calculated as the number of grid cells that sharks and fishing effort (in days) occurred in the same $1^\circ \times 1^\circ$ grid cells in an average month, as a function of all shark grid cells occupied and standardized for shark track length. This was summarized as spatial overlap (%) = $100(n_o/n_c)$, in which n_o is the number of grid cells occupied by an individual tracked shark that overlap with grid cells with fishing effort and n_c is the total number of grid cells occupied by an individual tracked shark. The mean monthly spatial overlap of an individual shark was determined from monthly spatial overlap values, and the mean monthly spatial overlap per species was calculated by averaging the mean monthly individual spatial overlap values across all individuals of a species within each ocean region. A fixed $1^\circ \times 1^\circ$ geographical grid cell (in which $1^\circ = 110.6$ km) was chosen, because it is the approximate length of high-seas longlines (that is, 100-km long with an average of 1,200 baited hooks⁵ that attract fish over long distances^{19,20}); because it was similar to the broad light-based geolocation error field of PSAT tags ($n = 615$ sharks; 37% of the total tracks) after SSM processing that we used here, generally shown to be about $0.4\text{--}1.5^\circ$ latitude (about $45\text{--}167$ km)^{32,44–46}; and because it exceeded the upper 95% confidence intervals of the mean daily movement distances of the widest-ranging sharks that we tracked (Supplementary Table 16). In addition, the $1^\circ \times 1^\circ$ grid-cell size was suitable to reduce the effects of gaps in AIS coverage that, at smaller grid sizes, could potentially result in substantial unrecorded fishing effort per grid cell^{19–23}. To examine the effect of grid-cell size on estimates of spatial overlap^{19,20,47}, we calculated the

overlap of all sharks tracked with ARGOS transmitters, from which locations estimated from SSMS were fitted to ARGOS observations (for example, 2.4–5.5-km spatial accuracy⁴⁸), with longline-fishing effort at 2° × 2°, 1° × 1°, 0.75° × 0.75°, 0.50° × 0.50°, 0.25° × 0.25° and 0.10° × 0.10° grid-cell sizes (Extended Data Fig. 4, Supplementary Fig. 4).

An estimate of the exposure of an individual shark to fishing effort within each grid cell occupied during its observed track was termed the FEI and calculated as:

$$FEI = \frac{\sum_{i=1}^n f_i d_i}{n} \quad (3)$$

Here FEI pertains to an individual shark per month in a given year. The term f_i is the fishing effort (number of vessel days) in grid cell i occupied by a shark during its track; d_i is the relative density contribution for all location estimates for an individual shark summed in grid cell i of its track (that is, location estimates of an individual shark were weighted by the inverse of the number of total individual sharks of a single species on the same relative day of their track, and with the weights for each species normalized to one; see ‘Spatial density analysis’); and n is the number of grid cells occupied by an individual shark during its track in a given month of a given year. Individual mean FEI was calculated for an individual shark by averaging the monthly FEI values of an individual shark through time (over the duration of its observed track in monthly steps). To estimate the typical exposure within a species, individual-species mean FEI was calculated by averaging individual-shark mean FEI values for that species within each ocean region (Figs. 3, 4).

To map the mean monthly spatial variation in overlap and fishing effort (fishing exposure) within the space used by sharks (Fig. 2c), we calculated the product of D_{it} and f_i in each grid cell in each month of a relative year across individual sharks (regardless of species), and averaged across the 12 months within each grid cell. In addition, for comparing temporally matched shark–vessel spatial overlap and fishing effort in 2012–2016, we repeated the calculation above but including only those individuals (species) present within these years by multiplication of f_i with the re-calculated D_{it} for those years only (see ‘Spatial density analysis’ for details).

To test for differences in the exposure risk of sharks to fishing activity between different species within the general fishing areas designated by the FAO (Extended Data Fig. 1c), we undertook statistical analysis of exposure risk calculated for each shark as the product of the mean monthly spatial overlap and mean monthly fishing effort. Because the data were not normal (Shapiro–Wilk normality test, $P < 0.05$), a Kruskal–Wallis test was performed (with pairwise Wilcoxon rank-sum tests as a post hoc test). Because of differences in the number of tagged individuals per species, groups of >25 sharks per species were randomly selected and the Kruskal–Wallis test performed. This procedure was repeated 1,000 times and the percentage of times that significant differences were observed was recorded. Species with fewer than 25 individuals tracked were removed from the analysis. Given the lower numbers of sharks tracked in the southwest Indian Ocean and Oceania regions (Supplementary Table 14), statistical tests were restricted to the North Atlantic Ocean and eastern Pacific Ocean regions. In the Atlantic Ocean, selected species were *P. glauca* ($n = 152$), *Isurus* spp. ($n = 120$), *G. cuvier* ($n = 131$), *C. carcharias* ($n = 26$), *C. longimanus* ($n = 99$), *L. nasus* ($n = 46$), *C. leucas* ($n = 38$) and *Sphyrna* spp. ($n = 40$); in the Pacific Ocean, species were *P. glauca* ($n = 112$), *I. oxyrinchus* ($n = 113$), *L. ditropis* ($n = 172$), *R. typus* ($n = 77$) and *C. carcharias* ($n = 59$).

Shark landings. Mean annual pelagic shark landings (t) by species/taxa groups were obtained from the FAO database (www.FAO.org/fishery/statistics/global-capture-production/query/en; downloaded September 2018) and related to the median monthly FEI of each species or taxa group. Landings reported for the North Atlantic Ocean (northwest, northeast, western central and eastern central Atlantic Ocean) between 2007 and 2016 were used in the analysis, because these spanned the main period during which most sharks were tracked (70% between 2007–2017) and longline-fishing effort was monitored (2012–2016). Data were extracted for eight species or taxa groups that are regularly caught by shelf and/or high-seas fisheries in the North Atlantic Ocean, the region in which most tags were deployed. The species and taxa groups were *P. glauca*, *I. oxyrinchus*, *C. longimanus*, *C. leucas*, *L. nasus*, *G. cuvier*, *C. carcharias* and hammerheads (*Sphyrna* spp., comprising *S. lewini*, *S. mokarran* and *S. zygaena*).

Reporting summary. Further information on research design is available in the Nature Research Reporting Summary linked to this paper.

Data availability

The source code used to undertake analyses and to prepare figures, in addition to the derived data underlying Fig. 2 maps (shark relative spatial density, longline-fishing effort and shark–longline-fishing overlap and FEI) and Fig. 3 plots (spatial overlap and FEI) is freely available on GitHub (<https://github.com/GlobalSharkMovement/GlobalSpatialRisk>).

32. Wilson, R. P., Ducamp, J.-J., Rees, W. G., Culik, B. M. & Niekamp, K. in *Wildlife Telemetry* (eds Priede, I. G. & Swift, S. M.) 131–134 (Ellis Horwood, Chichester, 1992).
33. Delong, R. L., Stewart, B. S. & Hill, R. D. Documenting migrations of northern elephant seals using day length. *Mar. Mamm. Sci.* **8**, 155–159 (1992).
34. Lam, C., Nielsen, A. & Sibert, J. Improving light and temperature based geolocation by unscented Kalman filtering. *Fish. Res.* **91**, 15–25 (2008).
35. Johnson, D. S., London, J. M., Lea, M.-A. & Durban, J. W. Continuous-time correlated random walk model for animal telemetry data. *Ecology* **89**, 1208–1215 (2008).
36. Sippel, T., Holdsworth, J., Dennis, T. & Montgomery, J. Investigating behaviour and population dynamics of striped marlin (*Kajikia audax*) from the southwest Pacific Ocean with satellite tags. *PLoS ONE* **6**, e21087 (2011).
37. Jonsen, I. D., Flemming, J. M. & Myers, A. E. Robust state-space modeling of animal movement data. *Ecology* **86**, 2874–2880 (2005).
38. Lunn, D. J., Thomas, A., Best, N. & Spiegelhalter, D. WinBUGS – a Bayesian modelling framework: 472 concepts, structure, and extensibility. *Stat. Comput.* **10**, 325–337 (2000).
39. Ward-Paige, C. A., Britten, G. L., Bethea, D. M. & Carlson, J. K. Characterizing and predicting essential habitat features for juvenile coastal sharks. *Mar. Ecol. (Berl.)* **36**, 419–431 (2014).
40. Queiroz, N. et al. Convergent foraging tactics of marine predators with different feeding strategies across heterogeneous ocean environments. *Front. Mar. Sci.* **4**, 239 (2017).
41. Fisher, R., Wilson, S. K., Sin, T. M., Lee, A. C. & Langlois, T. J. A simple function for full-subsets multiple regression in ecology with R. *Ecol. Evol.* **3**, 6104–6113 (2018).
42. Burnham, K. P. & Anderson, D. R. Multimodel inference: understanding AIC and BIC in model selection. *Sociol. Methods Res.* **33**, 261–304 (2004).
43. Wood, S. N. Fast stable restricted maximum likelihood and marginal likelihood estimation of semiparametric generalized linear models. *J. R. Stat. Soc. Series B Stat. Methodol.* **73**, 3–36 (2011).
44. Teo, S. L. H. et al. Validation of geolocation estimates based on light level and sea surface temperature from electronic tags. *Mar. Ecol. Prog. Ser.* **283**, 81–98 (2004).
45. Nielsen, A., Bigelow, K. A., Musyl, M. K. & Sibert, J. R. Improving light-based geolocation by including sea surface temperature. *Fish. Oceanogr.* **15**, 314–325 (2006).
46. Sims, D. W. in *Sharks and Their Relatives II – Biodiversity, Adaptive Physiology and Conservation* (eds Carrier, J. C. et al.) 351–392 (CRC, Boca Raton, 2010).
47. Amoroso, R. O., Parma, A. M., Pitcher, C. R., McConaughy, R. A. & Jennings, S. Comment on “Tracking the global footprint of fisheries”. *Science* **361**, eaat6713 (2018).
48. Lowther, A. D., Lydersen, C., Fedak, M. A., Lovell, P. & Kovacs, K. M. The Argos–CLS Kalman filter: error structures and state-space modelling relative to Fastloc GPS data. *PLoS ONE* **10**, e0124754 (2015).

Acknowledgements We thank all who were involved in fieldwork and data collection (full details are given in the Supplementary Information). Data analysis was funded in part by the Marine Biological Association (MBA) and the UK Natural Environment Research Council (NERC) (NE/R00997X/1) (to D.W.S.) with additional research support from the Save Our Seas Foundation and the NERC Oceans 2025 Strategic Research Programme, in which D.W.S. was a principal investigator. D.W.S. was supported by an MBA Senior Research Fellowship, N.Q. by European Regional Development Fund (FEDER) via the Programa Operacional Competitividade e Internacionalização (COMPETE), National Funds via Fundação para a Ciência e a Tecnologia (FCT) under PTDC/MAR/100345/2008 and COMPETE FCOMP-01-0124-FEDER-010580 (to N.Q. and D.W.S.), and Norte Portugal Regional Operational Programme (NORTE 2020) under the PORTUGAL 2020 Partnership Agreement through the European Regional Development Fund (ERDF) in project MarInfo (NORTE-01-0145-FEDER-000031). Additional support was provided by an FCT Investigator Fellowship IF/01611/2013 (N.Q.), FCT Doctoral Fellowship PD/BD/52603/2014 (M.V.), PTDC/MAR-BIO/4458/2012, Xunta de Galicia - Isabel Barreto Program 2009-2012 (G.M.), Australian Research Council (ARC) grant DE170100841 and operational funds from the Australian Institute for Marine Science (AIMS) (both to A.M.M.S.). We thank Stanford University, the Tagging of Pacific Predators programme and Global Fishing Watch for making data freely available. We thank M. Dando for creating the shark images. This research contributes to the Global Shark Movement Project (GSMP).

Author contributions The GSMP is coordinated by D.W.S. N.Q. and D.W.S. conceived the study, N.Q., N. E. Humphries and D.W.S. designed the study, and all authors contributed to animal tagging, fieldwork, data collection and/or contribution of tools (full details are given in the Supplementary Information). N.Q., N. E. Humphries, A.C., M.V., I.d.C., A.M.M.S., L.L.S., S.J.S. and D.W.S. analysed the collated data. D.W.S. drafted the paper with contributions from N.Q., N. E. Humphries and A.M.M.S. All authors contributed to subsequent drafts.

Competing interests The authors declare no competing interests.

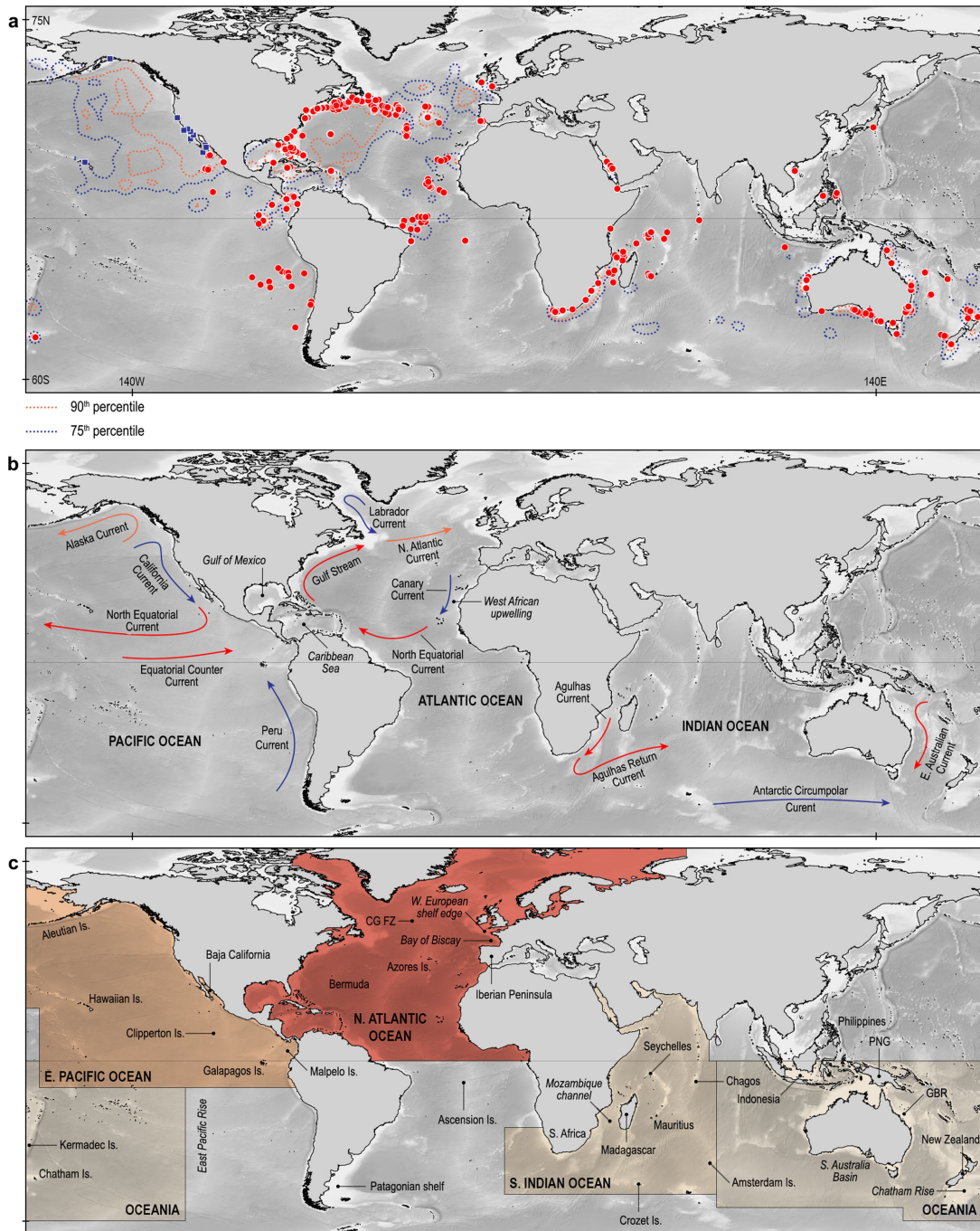
Additional information

Supplementary information is available for this paper at <https://doi.org/10.1038/s41586-019-1444-4>.

Correspondence and requests for materials should be addressed to D.W.S.

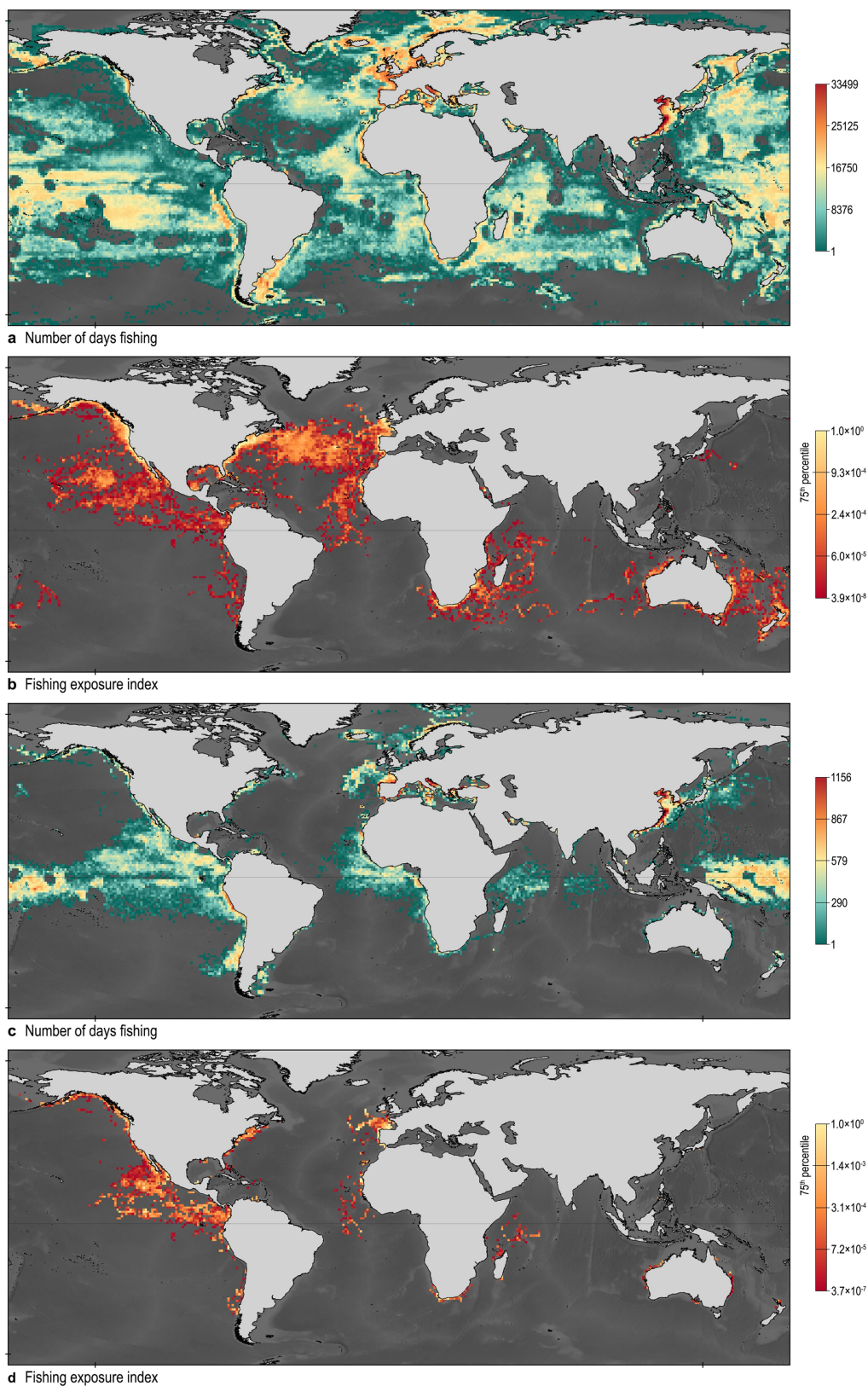
Peer review information Nature thanks Julia Baum, Brendan Godley, Ian Jonsen and David Kroodsma for their contribution to the peer review of this work.

Reprints and permissions information is available at <http://www.nature.com/reprints>.



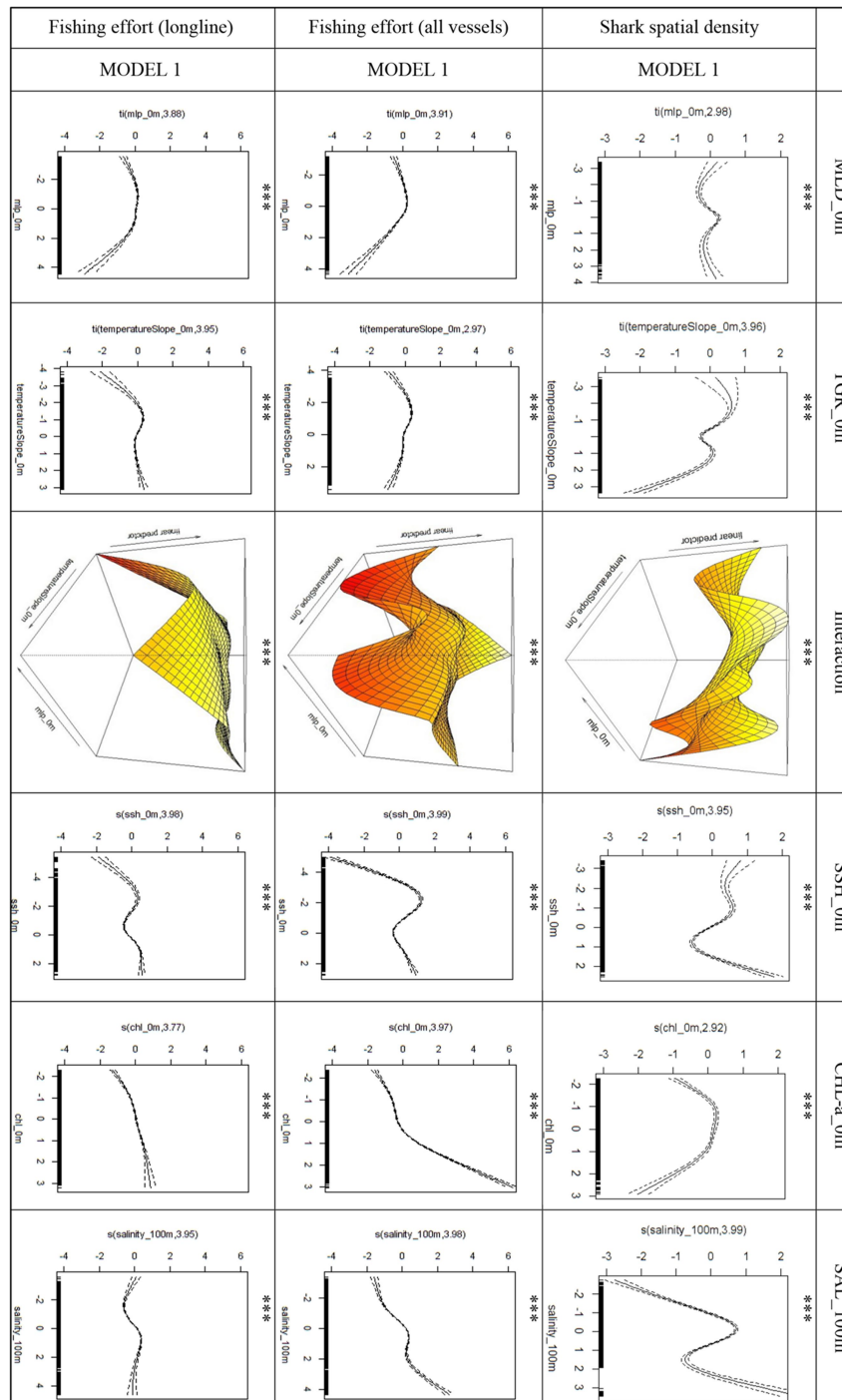
Extended Data Fig. 1 | The locations of shark tag deployment sites in relation to shark space-use hotspots, ocean currents, physical features and fishing areas. a, Red circles denote the locations in which satellite transmitters were attached and sharks released, and blue squares in the eastern Pacific Ocean denote the annual median deployment locations of tags by the TOPP program¹¹. Shark space-use hotspots are shown as the 75th (blue dotted lines) and 90th percentiles (red dotted lines) of the mean

monthly relative density of estimated shark locations within $1^\circ \times 1^\circ$ grid cells given in Fig. 2a. **b, c,** Schematic maps of major ocean currents (**b**) and physical features overlaid on FAO fishing areas (**c**). Coloured arrows in **b** denote the thermal regime of currents, with warmer colours indicating higher water temperatures. CGFZ, Charlie Gibbs Fracture Zone; GBR, Great Barrier Reef; PNG, Papua New Guinea.



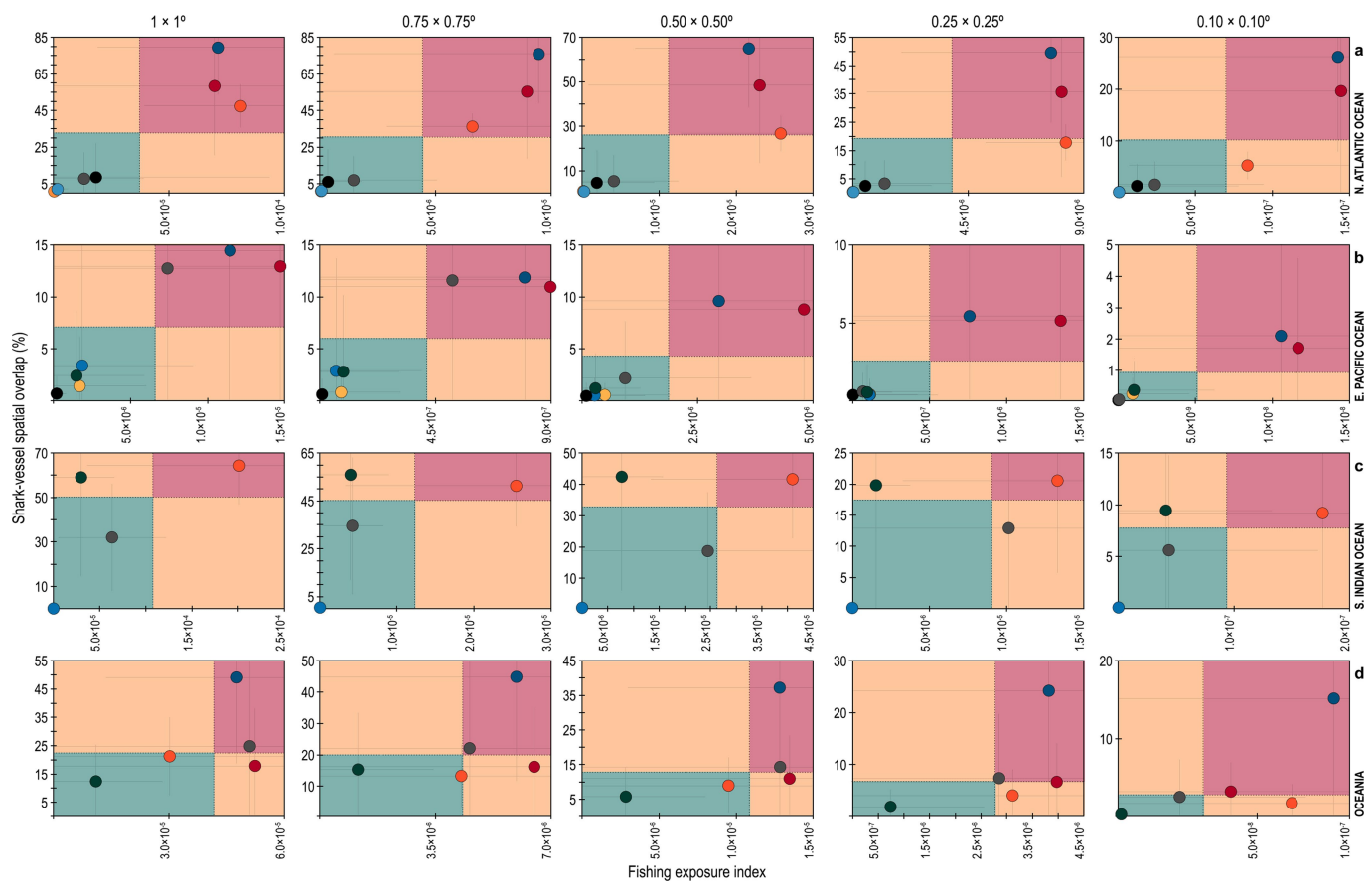
Extended Data Fig. 2 | Spatial distribution of fishing vessels and overlap with sharks. **a**, Distribution of the fishing effort of AIS-tracked vessels (mean annual days spent per grid cell) between 2012 and 2016 (Methods). **b**, Distribution of the mean monthly overlap and level of the fishing effort for all vessels (in days) to which sharks were exposed in overlapping areas, for all species, within $1^\circ \times 1^\circ$ grid cells (Methods). Spatial overlap hotspots were defined as $1^\circ \times 1^\circ$ grid cells with ≥ 75 th percentile of mean FEI. Note that the overlap pattern of sharks and all mapped AIS-equipped fishing

vessels is similar to that determined for sharks and longline-fishing vessels in Fig. 2c. **c**, Distribution of the fishing effort of AIS-equipped purse-seine vessels, using mean annual days spent per grid cell between 2012 and 2016 (Methods). **d**, Distribution of the mean monthly overlap and level of fishing effort of purse-seine vessel (in days) to which sharks were exposed in overlapping areas, for all species, within $1^\circ \times 1^\circ$ grid cells (Methods). Spatial overlap hotspots were defined as $1^\circ \times 1^\circ$ grid cells with ≥ 75 th percentile of mean FEI.



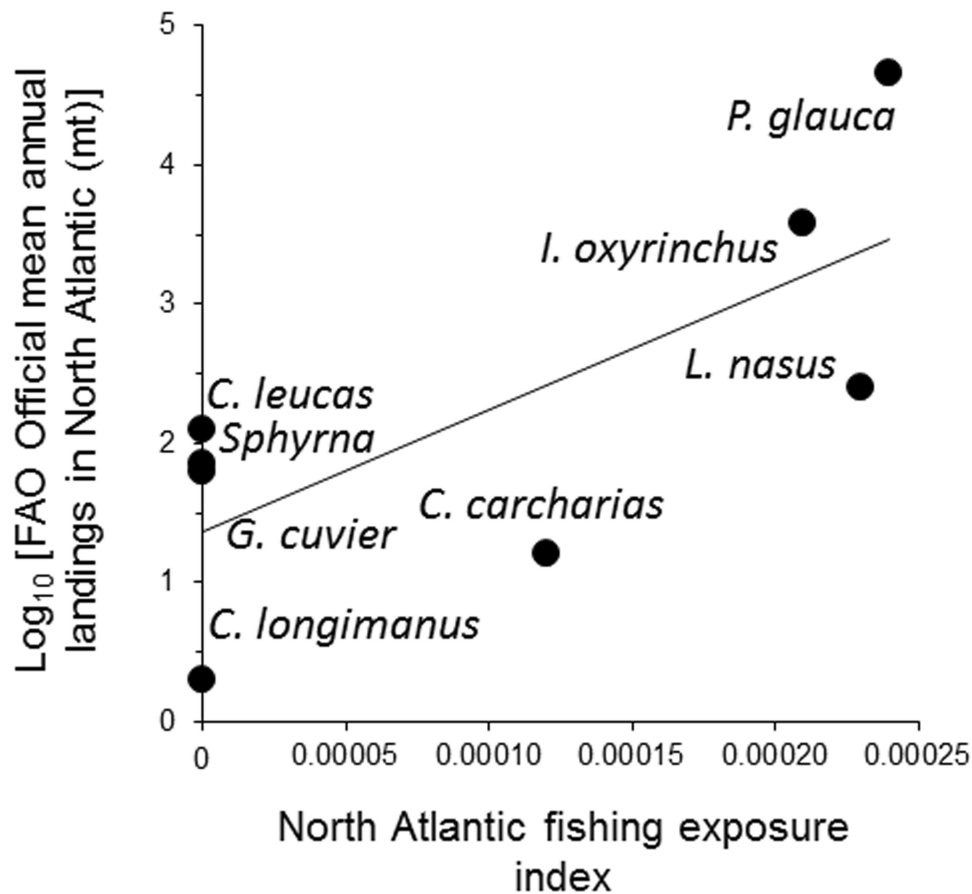
Extended Data Fig. 3 | Environmental modelling results. Estimated relationships between mean monthly relative density of all sharks (top) and fishing effort of all AIS-equipped fishing vessels (middle) and longline-fishing vessels only (bottom), with all environmental variables in

the highest-ranked model (model 1) of the GAM tested. The third column shows the interaction results between the two variables described in the first and second columns. Asterisks indicate the significance level for each smooth term included in the GAM; *** $P < 0.001$.



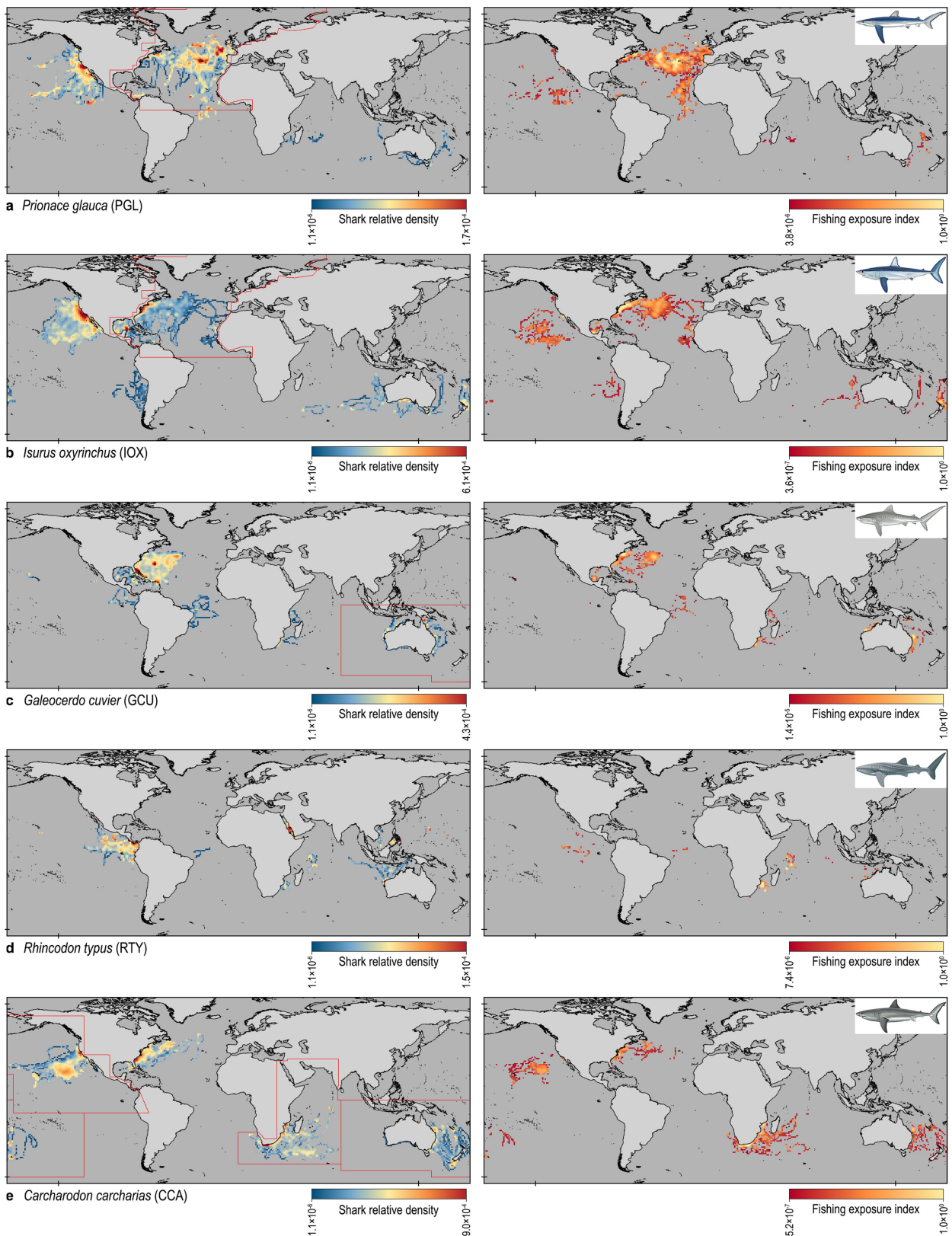
Extended Data Fig. 4 | Effect of grid-cell size on risk-exposure patterns of sharks to longline fisheries. a–d, North Atlantic Ocean (a), east Pacific Ocean (b), southwest Indian Ocean (c) and Oceania (d). Note that, regardless of the grid-cell size at which the individual-species mean spatial overlap and FEI were calculated, the species that occur in the highest- (red) and the lowest-risk zones (green) remain notably conserved, which indicates a general pattern that is not dependent on the scale at which

these data were analysed. Shark-species identification codes corresponding to marker colours are given in Fig. 3. In addition, for the North Atlantic (a), hammerhead sharks (*Sphyrna* spp.) are represented by a black circle and oceanic whitetip sharks (*C. longimanus*) by a light blue circle; for the eastern Pacific Ocean (b), the salmon shark (*L. ditropis*) is represented by a light orange circle. Error bars are ± 1 s.d. An additional comparison of $2^\circ \times 2^\circ$ with $1^\circ \times 1^\circ$ grid-cell size is given in Supplementary Fig. 4.



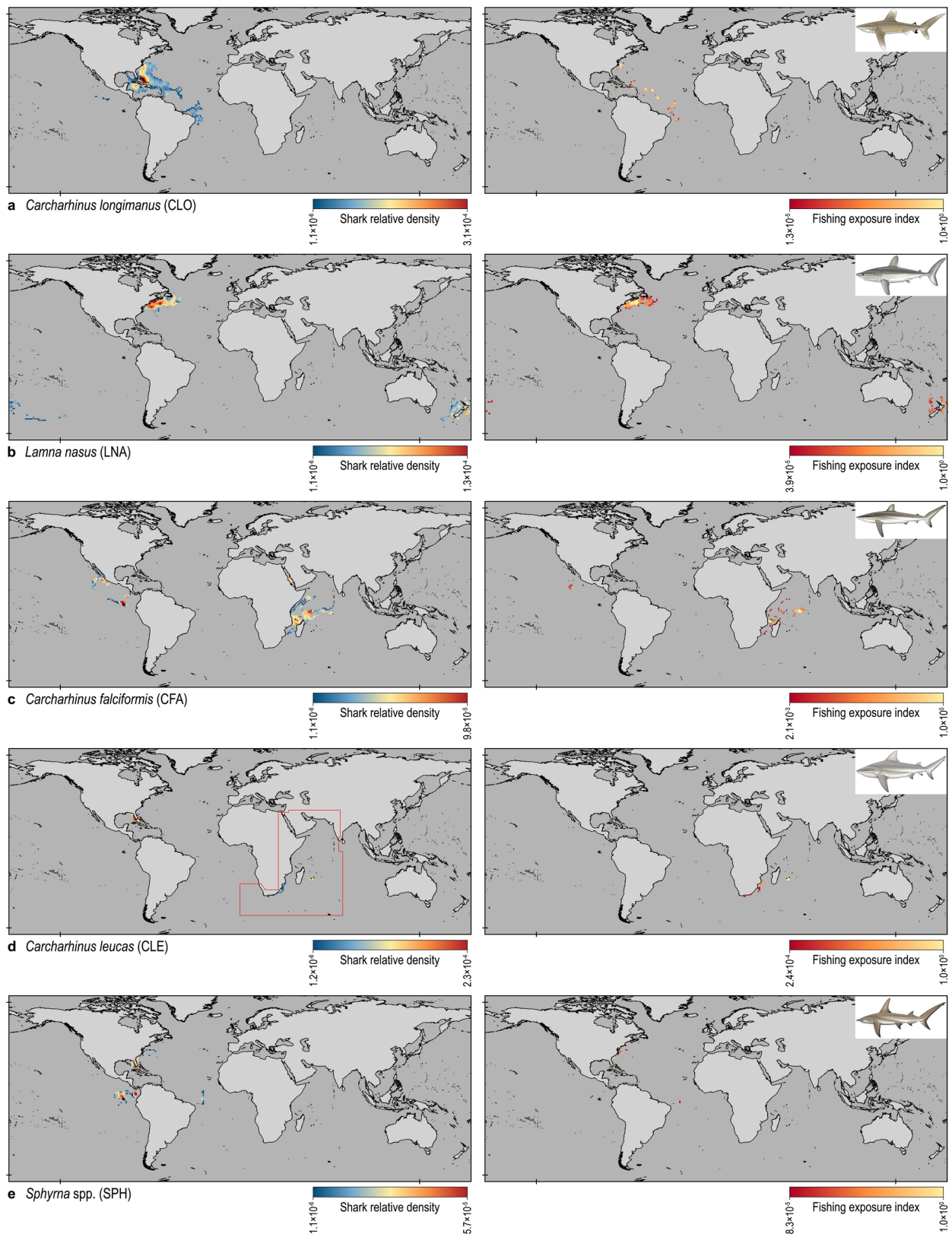
Extended Data Fig. 5 | Relationship between shark landings by fisheries in the North Atlantic Ocean, and shark density–longline FEI. Plot showing shark landings from the North Atlantic Ocean (mean, 2007–2016), extracted from the FAO total-capture production database, was dependent upon the longline-fishing effort in the North Atlantic Ocean, as estimated with the individual-species FEI (70% of sharks tracked, 2007–2017; AIS data, 2012–2016) (Methods).

Using linear regression, we tested the null hypothesis (H_0) that $\beta = 0$ after normalizing landings (in metric tonnes) by log-transformation and for median FEI per species. Regression analysis gave the equation: $\log(\text{landings}) = 1.364 + 8,732 \text{ FEI}$, with a regression coefficient (b) standard error of 3,369. We computed $r^2 = 0.45$, $F = 6.72$ and $F_{0.05(1),1.7} = 5.59$, therefore rejecting H_0 at the 5% level of significance with $P < 0.05$.



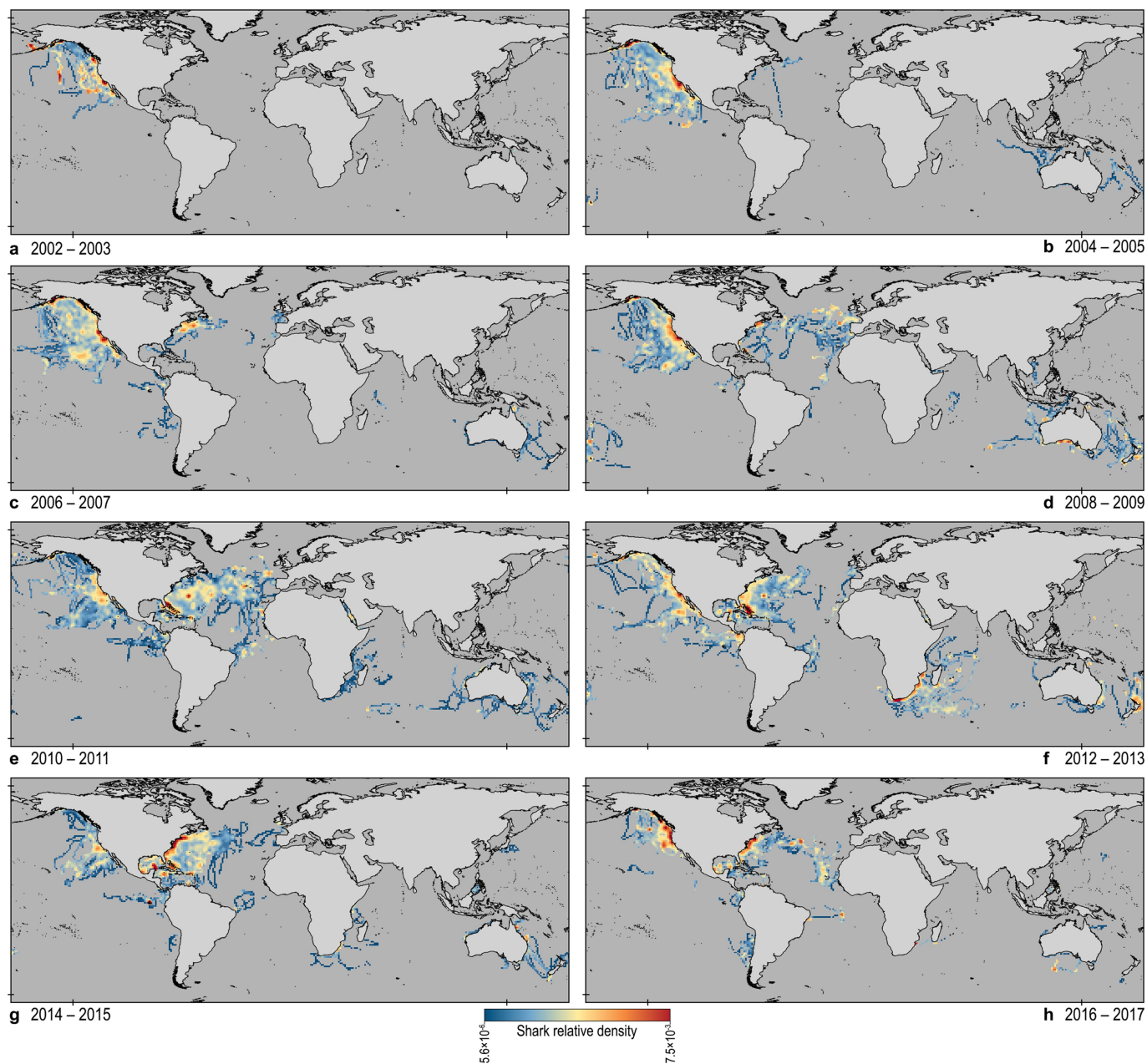
Extended Data Fig. 6 | Relative density and spatial overlap distributions for the five most data-rich individual shark species that occur in multiple oceans. a–e, Mean monthly relative density of shark species (left) tracked in 2002–2017 in comparison with species-mean FEI per grid

cell (right) for the 5 most data-rich species or taxa groups that occur in multiple oceans: blue shark (a), shortfin mako shark (b), tiger shark (c), whale shark (d) and white shark (e). Red boxes denote areas shown in Fig. 3. Shark images created by M. Dando.



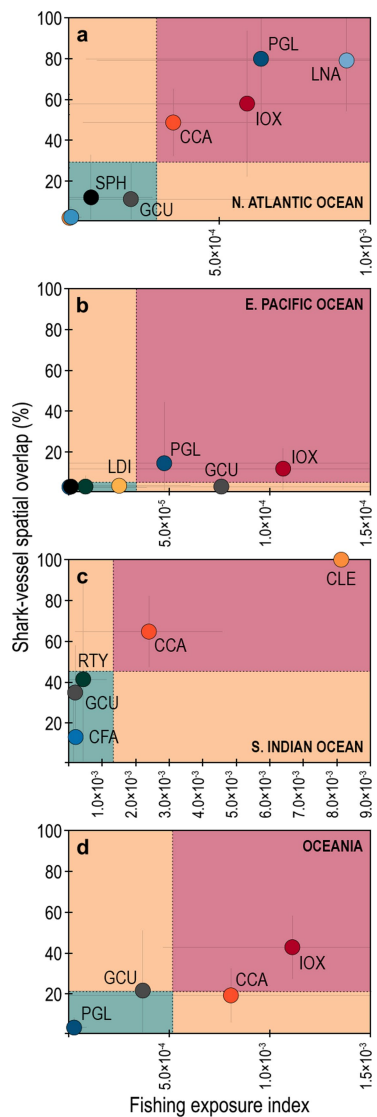
Extended Data Fig. 7 | Relative density and spatial overlap distributions for the sixth to tenth most data-rich individual shark species that occur in multiple oceans. Mean monthly relative density of shark species (left) tracked in 2002–2017 in comparison with species-mean FEI per grid cell (right) for the sixth to tenth most data-rich species or taxa groups that

occur in multiple oceans: oceanic whitetip shark (a), porbeagle shark (b), silky shark (c), bull shark (d) and hammerhead sharks (d) (comprising the scalloped hammerhead shark, the great hammerhead shark and the smooth hammerhead shark). Shark images created by M. Dando. CLO, *Carcharhinus longimanus*; SPH, *Sphyrna* spp.

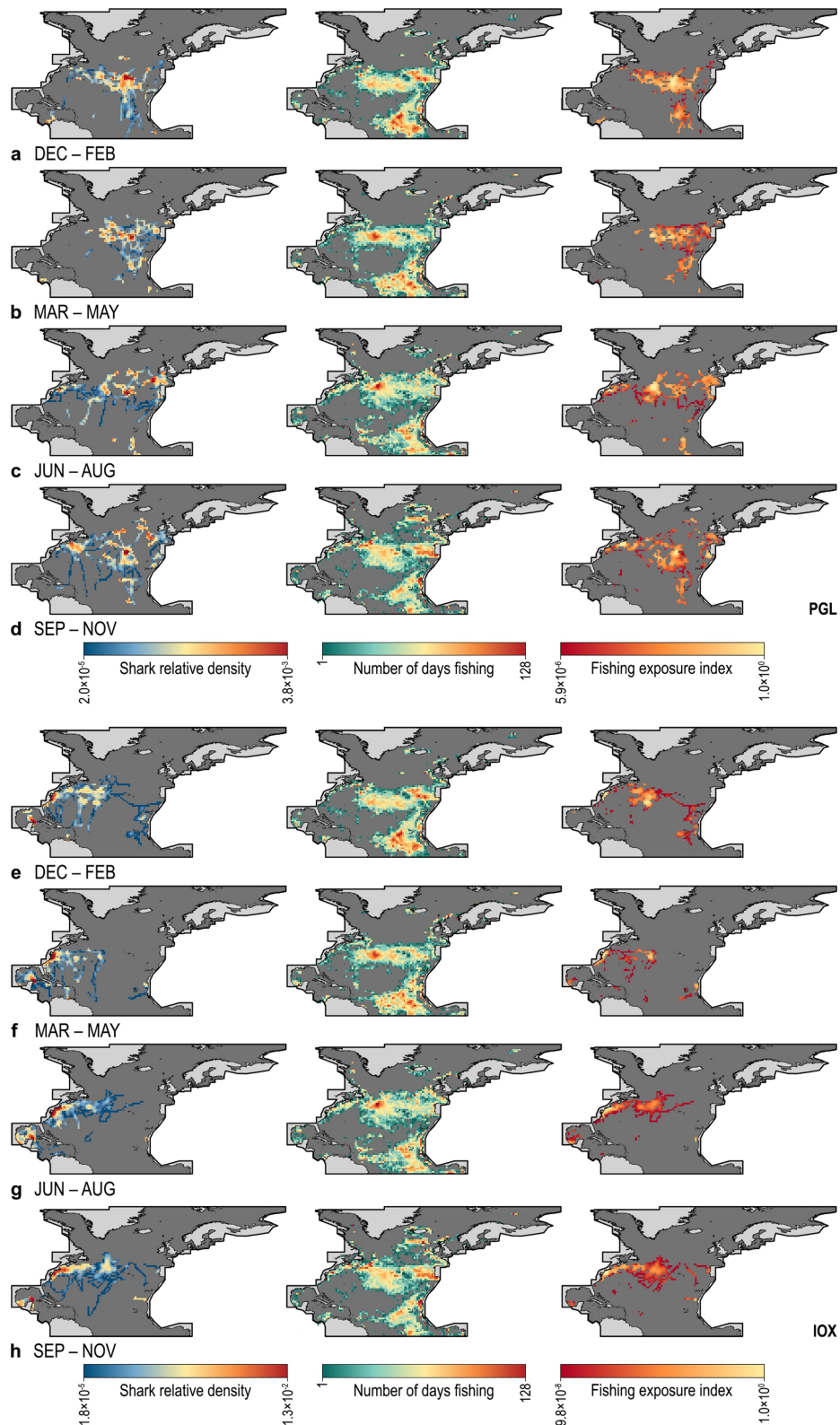


Extended Data Fig. 8 | Between-years patterns in global spatial density of pelagic sharks. Mean monthly spatial density was calculated for each two-year period across species. We used consecutive two-year groups to reduce gaps in coverage. Note that there were broad-scale shark tracks in the east Pacific Ocean in all eight two-year periods (2002–2003 to 2016–2017), in the North Atlantic Ocean between 2006–2007 and

2016–2017, in the southwest Indian Ocean in 2010–2011 to 2014–2015, and in Oceania between 2004–2005 and 2014–2015. This indicates that temporal consistency of shark tracks was present within the ocean regions studied, which suggests that the spatial hotspots that we identified are more likely to be persistent between years.



Extended Data Fig. 9 | Risk-exposure patterns of sharks from longline fisheries between 2012 and 2016. a–d, North Atlantic Ocean (a), east Pacific Ocean (b), southwest Indian Ocean (c) and Oceania (d). Note that species patterns of exposure to risk in highest-risk (red) and lowest-risk (green) zones in the years 2012–2016, which matched shark density data with longline-fishing effort data from AIS-equipped vessels directly, were very similar to patterns found for shark density (2002–2017) and longline-fishing effort data from AIS-equipped vessels (species-mean FEI) (2012–2016) (shown in Fig. 3), which indicates that there was no important effect of temporally mismatched datasets on the results. LDI, *L. ditropis*.



Extended Data Fig. 10 | Seasonal shifts in sharks, longline-fishing vessels and patterns of overlap with fishing effort. a–h, Mean quarterly relative spatial density of sharks (left), longline-fishing effort (in days) (middle) and mean FEI per grid cell (the fishing effort to which sharks were exposed in overlapped areas) (right) for blue sharks in the

North Atlantic Ocean in December–February (a), March–May (b), June–August (c) and September–November (d), and for shortfin mako sharks in the North Atlantic Ocean in December–February (e), March–May (f), June–August (g) and September–November (h).

Reporting Summary

Nature Research wishes to improve the reproducibility of the work that we publish. This form provides structure for consistency and transparency in reporting. For further information on Nature Research policies, see [Authors & Referees](#) and the [Editorial Policy Checklist](#).

Statistical parameters

When statistical analyses are reported, confirm that the following items are present in the relevant location (e.g. figure legend, table legend, main text, or Methods section).

n/a Confirmed

- The exact sample size (n) for each experimental group/condition, given as a discrete number and unit of measurement
- An indication of whether measurements were taken from distinct samples or whether the same sample was measured repeatedly
- The statistical test(s) used AND whether they are one- or two-sided
Only common tests should be described solely by name; describe more complex techniques in the Methods section.
- A description of all covariates tested
- A description of any assumptions or corrections, such as tests of normality and adjustment for multiple comparisons
- A full description of the statistics including central tendency (e.g. means) or other basic estimates (e.g. regression coefficient) AND variation (e.g. standard deviation) or associated estimates of uncertainty (e.g. confidence intervals)
- For null hypothesis testing, the test statistic (e.g. F , t , r) with confidence intervals, effect sizes, degrees of freedom and P value noted
Give P values as exact values whenever suitable.
- For Bayesian analysis, information on the choice of priors and Markov chain Monte Carlo settings
- For hierarchical and complex designs, identification of the appropriate level for tests and full reporting of outcomes
- Estimates of effect sizes (e.g. Cohen's d , Pearson's r), indicating how they were calculated
- Clearly defined error bars
State explicitly what error bars represent (e.g. SD , SE , CI)

Our web collection on [statistics for biologists](#) may be useful.

Software and code

Policy information about [availability of computer code](#)

Data collection

Shark satellite tracking: Raw location data from pop-off satellite archival transmitters (PSATs) processed after ARGOS satellite acquisition using tag manufacturers custom software (Wildlife Computers; Microwave Telemetry; Desert Star Systems) to calculate latitude and longitude. Raw positions processed using a UKFSST state space model (UKFSST R package). Raw ARGOS tag locations after satellite acquisition were processed with a speed filter (in R). For both tag types (PSAT and ARGOS), daily time series of locations estimated using a continuous time correlated random walk (CTCRW) Kalman filter (crawl R package). TOPP tag data was filtered with a Bayesian based state space model using WinBugs (for priors and MCMC sampling see Methods).
Fishing vessel tracking: Processed data were acquired from the Global Fishing Watch. for code and processing details see ref. 19 in paper.

Data analysis

R, Minitab v18 and ArcGIS

For manuscripts utilizing custom algorithms or software that are central to the research but not yet described in published literature, software must be made available to editors/reviewers upon request. We strongly encourage code deposition in a community repository (e.g. GitHub). See the Nature Research [guidelines for submitting code & software](#) for further information.

Data

Policy information about [availability of data](#)

All manuscripts must include a [data availability statement](#). This statement should provide the following information, where applicable:

- Accession codes, unique identifiers, or web links for publicly available datasets
- A list of figures that have associated raw data
- A description of any restrictions on data availability

The source code used to undertake analyses and to prepare figures, in addition to the derived data in spreadsheet form underlying Fig. 2 maps (shark relative spatial density; longline fishing effort; and shark– longline overlap and FEI) and Fig. 3 plots (spatial overlap and FEI) are freely available to download on GitHub (github.com/GlobalSharkMovement/GlobalSpatialRisk). Processed fishing vessel effort data are available to download at <http://globalfishingwatch.org/datasets-and-code/>

Field-specific reporting

Please select the best fit for your research. If you are not sure, read the appropriate sections before making your selection.

Life sciences Behavioural & social sciences Ecological, evolutionary & environmental sciences

For a reference copy of the document with all sections, see nature.com/authors/policies/ReportingSummary-flat.pdf

Ecological, evolutionary & environmental sciences study design

All studies must disclose on these points even when the disclosure is negative.

Study description	The study describes the distributions of satellite tracked pelagic sharks and fishing vessels across the global oceans and calculates the extent of overlap and fishing effort different shark species are exposed to in space and time. See Methods for time periods of data collection.
Research sample	Movements of individual pelagic sharks were satellite tracked (n = 1804) from 23 threatened species in the Atlantic, Pacific and Indian oceans. Species details including number and locations of tags deployed on each species are given in the paper. Fishing vessels (n > 80,000) were tracked globally using the automatic identification system. These data were downloaded from Global Fishing Watch.
Sampling strategy	Pelagic sharks were captured alive at sea with baited hooks or with purse seines prior to tagging and subsequent release. Some sharks were tagged while free swimming. Tags were fitted externally within a few minutes. Tagging was undertaken by 30 different research groups across many countries with tagging procedures approved by institutional ethical boards and conforming to national regulations.
Data collection	Each research group collected shark track data independently by download from the ARGOS satellite service provider.
Timing and spatial scale	Pelagic sharks were tracked between 2002 and 2017. Details of tag deployments and tracking durations are detailed in the paper.
Data exclusions	Poor quality data were reported for 123 tags (72 ARGOS and 51 PSATs) due to early tag failure, premature tag pop-off and/or a high percentage of locations estimated with high spatial error, e.g. raw computed geolocations over land, all of which resulted in poor state space model fits and hence short or unreliable track reconstructions. These data were excluded.
Reproducibility	No experiments as such were conducted, rather our data are based on satellite tracked movements of individual pelagic sharks and fishing vessels.
Randomization	Randomization procedures were used and are fully described in the Methods and Supplementary Information files.
Blinding	Blinding is not relevant to this type of study because data are based on movements of wild animals and fishing vessels.
Did the study involve field work?	<input checked="" type="checkbox"/> Yes <input type="checkbox"/> No

Field work, collection and transport

Field conditions	Tags were deployed on pelagic sharks in the Atlantic, Pacific and Indian Oceans under a range of conditions.
Location	Locations of tagging and subsequent tracks of sharks are detailed in the paper (Fig. 1; Extended Data Fig. 1).
Access and import/export	No collections or import or export of samples was undertaken.
Disturbance	Disturbance to individual shark behaviour was minimised through completion of tagging procedures within a few minutes if captured, or during free swimming. All procedures were approved by institutional and national ethical review committees.

Reporting for specific materials, systems and methods

Materials & experimental systems

n/a	Involvement	Involved in the study
<input checked="" type="checkbox"/>	<input type="checkbox"/>	Unique biological materials
<input checked="" type="checkbox"/>	<input type="checkbox"/>	Antibodies
<input checked="" type="checkbox"/>	<input type="checkbox"/>	Eukaryotic cell lines
<input checked="" type="checkbox"/>	<input type="checkbox"/>	Palaeontology
<input type="checkbox"/>	<input checked="" type="checkbox"/>	Animals and other organisms
<input checked="" type="checkbox"/>	<input type="checkbox"/>	Human research participants

Methods

n/a	Involvement	Involved in the study
<input checked="" type="checkbox"/>	<input type="checkbox"/>	ChIP-seq
<input checked="" type="checkbox"/>	<input type="checkbox"/>	Flow cytometry
<input checked="" type="checkbox"/>	<input type="checkbox"/>	MRI-based neuroimaging

Animals and other organisms

Policy information about [studies involving animals](#); [ARRIVE guidelines](#) recommended for reporting animal research

Laboratory animals

N/A

Wild animals

Satellite tags were fitted to individuals from 23 species of pelagic shark when captured or free swimming. Detailed information is provided in the Methods. All captured sharks were released after tag attachment. None were killed as part of the study. Tag release locations are given in Extended Data Fig. 1.

Field-collected samples

N/A